JPL 5105-9

Solar Thermal Power Systems Project
Parabolic Dish Power Systems
Research and Advanced Development

Analytical Foundations/Computer Model for Dish-Brayton Power System

D. P. Maynard
B. C. Gajanana

September 1980

Prepared for
U.S. Department of Energy
Through an agreement with
National Aeronautics and Space Administration
by
Jet Propulsion Laboratory
California Institute of Technology
Pasadena, California

5105-9
Solar Thermal Power Systems Project
Parabolic Dish Power Systems
Research and Advanced Development

Analytical Foundations/Computer Model for Dish-Brayton Power System

D. P. Maynard
B. C. Gajanana

September 1980

Prepared for
U.S. Department of Energy
Through an agreement with
National Aeronautics and Space Administration
by
Jet Propulsion Laboratory
California Institute of Technology
Pasadena, California

Prepared by the Jet Propulsion Laboratory, California Institute of Technology, for the U.S. Department of Energy through an agreement with the National Aeronautics and Space Administration.

The JPL Solar Thermal Power Systems Project is sponsored by the U.S. Department of Energy and forms a part of the Solar Thermal Program to develop low-cost solar thermal and electric power plants.

ABSTRACT

Analytical foundations are laid down for evaluating the performance of dish-Brayton power systems. The dish-Brayton power system analyzed here included three subsystems as part of the system: collector, receiver, and engine. This groundwork includes various assumptions and approximations that were used in developing the subsystem models and integrating them to a system model. Such a system model, apart from being able to evaluate the performance of the system, can be used in analyzing the system to delineate the effect of possible advanced technology improvements on overall system performance.

Based on the above analytical foundations, models are developed for collector, receiver, and engine subsystems. These models are integrated via a computer code to obtain a system model of the dish-Brayton power module. The design variables and operating variables of the various components are used as input to the model. The model evaluates system efficiency in terms of subsystem characteristics and determines optimum system efficiency for each set of subsystem characteristics.

The computer model is structured such that the various operating conditions and the component variables are input to the code. This flexibility of the computer code is well suited for performing a sensitivity analysis which will show the effect of input variables on system efficiency. Such an analysis is expected to indicate those areas of the power system which have greatest potential for system efficiency improvement.

ACKNOWLEDGMENTS

This report presents interim results of a study of the high-temperature dish-Brayton systems. The work was performed in the Advanced Systems Definition Task of the Parabolic Dish Power Systems Project, at the Jet Propulsion Laboratory, Pasadena, California, for the United States Department of Energy, via an interagency agreement with the National Aeronautics and Space Administration.

The authors would like to take this opportunity to express appreciation for contributions made by several individuals. Dr. N. R. Moore collaborated on the performance of this study throughout its duration and his contributions and guidance were essential. Dr. R. O. Hughes provided valuable technical assistance particularly in the area of the collector characterization. The computer programming and initial execution of the simulation code was handled by Iffat Khan. Wesley Menard reviewed the draft and offered valuable suggestions. The planning and direction of this work was competently performed by Toshio Fujita.

CONTENTS

Figures

SECTION I

INTRODUCTION

This report presents the analytical foundations that are required for evaluating the performance of a dish-Brayton system (DBS). These foundations are the basis for developing a computer model which is capable of simulating steady-state performance of the dish-Brayton system. The dish-Brayton system studied in this work consists of the following three elements:

(1) Point-focusing parabolic dish concentrator

(2) Cavity receiver

(3) Brayton cycle engine (gas turbine)

The point-focusing parabolic dish concentrator (henceforth referred to as dish) system consists of a reflective surface for focusing the incident solar insolation (sunlight), a structure to support the reflective surface and a tracking mechanism. Due to imperfections of the dish surface, the reflected insolation at the focus will be spread over a larger area than that of a perfect optical surface. A cavity receiver located at the focus of the dish collects this reflected insolation. The reflected solar energy enters the receiver cavity through a circular aperture which is located at the the focal plane of the dish. The solar energy collected by the cavity receiver is transferred to the Brayton engine through a heat exchanger located in the receiver. Depending on the type of gas turbine utilized (open or closed cycle) the same heat transfer fluid may be used as working fluid for the engine. This thermal energy drives the Brayton engine which in turn drives a generator or an alternator to produce electricity.

The Brayton cycle engines are very well suited for applications with dish systems from two considerations: high performance of the Brayton engine at elevated temperatures, and compactness of the Brayton engine for a given rating. The dish system has high optical collection efficiency and high temperature attainability; this suits the Brayton engine well. In the past, the development of smaller sized (below 150 hp) Brayton engine has been hindered by the lower performance of the engine due to leakage and pressure losses. Also, operating temperatures were limited since blade cooling techniques were not considered to be practical for small engines. Follow on studies to be made with the computer model are expected to point out the potential for improving the performance of small Brayton engines in terms of improved component performance and operation at higher temperatures through use of ceramic materials.

The study includes the thermodynamic analysis of the various components which compose the power system. The approach which has been adopted in this analysis has been to create a parametric characterization of the various system components. The parametric

characterization was then used to develop a model which simulates the thermodynamic performance of the system. This will allow the component characteristics of the power system tobe individually optimized in order to identify the best combined system performance where the system model accounts for the interactions among components. The results of this activity allow a sensitivity analysis to be performed which will determine the most potentially productive areas for future research and development activity. The computer model developed in this study is capable of evaluating the performance of both the open and closed Brayton cycle system with a variety of working fluids.

SECTION II

CONCENTRATOR CHARACTERIZATION

A. OVERVIEW

The concentrator reflects the sun's energy toward its focal point where the concentrated solar energy will enter the receiver and be available for conversion into useful work. The performance of the solar receiver at a specified receiver temperature, as measured either in terms of useful output or efficiency, improves with increases in the quantity of energy which it receives from the concentrator. Furthermore,it has been found that the quality of the concentrator reflecting surface is the predominant factor which governs receiver reradiation losses; a high quality surface is able to reflect the flux through a small receiver aperture having corresponding small reradiation losses.

A point-focusing parabolic dish has been selected as the type of solar concentrator to be evaluated in this study. This type of collector is well suited for operation with a gas turbine due to its high optical collection efficiency and ability to produce high temperatures. These high temperatures are ideally suited to the Brayton engine which requires high temperature for efficient operation. Point-focusing parabolic dish concentrators possess stringent pointing accuracy requirements which necessitate that such a system be equipped with a control system capability of two-axis tracking of the sun to ensure the correct orientation of the sun dish relative to the sun in order to obtain the maximum solar radiation.

This section of the report will describe the method by which the quantity of solar energy that will enter the receiver from the concentrator is determined. For the purpose of assisting in this description, a simplified sketch of the collector system is shown in Figure 2-1. A solar collector is defined as being comprised of a concentrator and a receiver as well as their attendant foundation, structure, and control mechanism.

B. FLUX DISTRIBUTION

A point focusing solar concentrator receives solar energy (insolation) from the sun and produces an intensified solar flux distribution at the focal plane of the concentrator. In this study a representative value of 800 W/m^2 or 74.324 W/ft^2 is used for the insolation incident on the concentrator.

The approach used in this analysis assumes that a radially symmetric solar flux distribution is produced at the concentrator focal plane as a result of the sun's finite image and the various reflector errors. The definition of a radially symmetric distribution is one that is a function only of the radial distance from its center

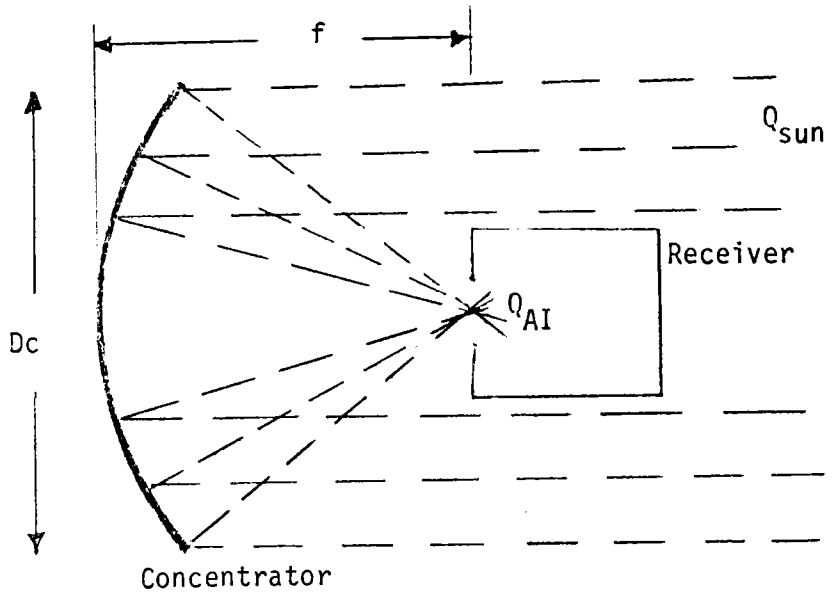

Figure 2-1 Simplified Sketch of Solar Collector

and is not dependent upon the angular displacement. Consequently any slice through the center of the flux distribution will be identical with any other slice. Furthermore if a relatively high quality concentrator is aimed directly at the sun, the resultant flux distribution tends to be approximately Gaussian with a standard deviation of σ_G. Since the assumption of a Gaussian flux distribution is accepted fairly extensively in the literature and greatly simplifies the analysis, it is henceforth employed in this study.

The most significant parameter which affects the flux distribution is the slope error of the concentrator which can be related to the standard deviation σ_G. This aspect will be dealt with later in this report.

The quantity of concentrated solar energy which is represented by the flux distribution is a function of the insolation, INS, incident upon the concentrator, the concentrator surface area (A_c), and the solar reflectivity of the concentrator surface (ρ_c) and can be expressed by the following equation:

$$Q_{con} = (INS)\ (A_c)\ (\rho_c)$$

By using the previously given value for the insolation, a 10 meter parabolic dish with a surface reflectivity of 0.8 has a value of Q_{con} equal to 50,265 watts. Having evaluated Q_{con}, the next essential step is the determination of the quantity of concentrated solar energy, Q_{AI}, which is accepted by the receiver located at the focal plane of the concentrator. By momentarily ignoring the presence of tracking and reflecting errors, it can be seen that if the radius of the receiver aperture is quite large, say $3\sigma_G$ to $4\sigma_G$ where σ_G was previously defined as a standard deviation of the Gaussian flux

distribution, then virtually all of the concentrated energy will be received. However, if the aperture radius is small, say 1 σ_G, or if the flux distribution is not centered in the aperture of the receiver (due to pointing errors), then the total received energy, Q_{AI}, will be noticeably less than Q_{con}.

The relationship of Q_{con} and Q_{AI} as a function of the solar flux distribution is shown in Figure 2-2 in terms of the dimensionless parameter, RA/DC, where RA is the radius of the receiver aperture and DC is the concentrator dish diameter.

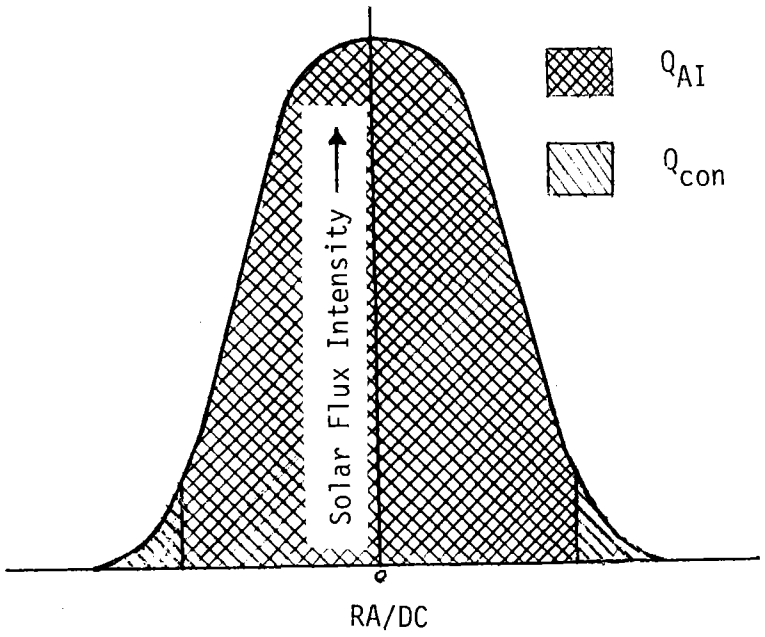

Figure 2-2 Solar Flux Distribution

C. OPTICAL ERROR

As was previously mentioned, optical errors which are a result of imperfect concentrator reflective surfaces are the predominant factors to be considered in the production of the focal plane solar flux distribution. Consequently the quality of the concentrator reflecting surface tends to be an important factor which influences the cost of the concentrator since the surface accuracy is governed by manufacturing tolerance which is in turn directly related to the construction cost.

These optical errors include slope errors, contour errors, and specular errors. Slope errors are defined as relatively small local deviations in the slope of the reflective surface. Contour errors are larger deviations than slope errors and are usually a result of inadequate structural support or dynamic deflections. Specular errors have the effect of spreading the concentrated light beams and are a

result of the quality of the reflective material which is utilized. The surface error of the reflective surface is defined as the angular deviation of the surface normal from that of a perfect geometry; it includes both the slope errors and the contour errors.

The primary effect which results from these errors is the spreading of the solar flux distribution which is generated at the focal plane of the concentrator. Consequently as the flux distribution is enlarged, a greater receiver aperture is necessary in order to gather a given percentage of the total flux and the geometric concentration ratio (concentrator area/receiver aperture area) of the collector is reduced.

The literature illustrates that, because of the highly interactive relationship between the quality of the concentrator and the characteristics of the heat engine, any reduction of the optical surface errors always results in an improvement of the performance of the system. Furthermore the performance improvement becomes more significant as the temperature increases.

The previous work performed by Hughes (Ref. 1 and 2) and Poon (Ref. 3) was essential in analytically determining the effect of the reflective surface slope error upon the quantity of concentrated solar flux which is gathered through the receiver aperture. Their work consisted essentially of the following basic steps:

(1) The solar flux intensity for various concentrator slope errors, σs, was plotted against radial distance normalized to concentrator diameter ratio, (RA/DC).

(2) These plots of flux distribution were curve-fitted in order to obtain the normalized Gaussian flux distribution and to determine the standard deviation, σ_G.

(3) The values for σ_G were then used to calculate the intercept factor (ϕ).

The effect of specular spreading can be included in the calculation of intercept factor by using an equivalent error. This equivalent error is calculated by (Ref. 9):

$$\sigma_{eq} = \sqrt{\sigma_s^2 + \sigma_{sp}^2/4}$$

where:

σ_{sp} = specular spreading error

σ_{eq} = equivalent error

To include the specular spreading effect in the calculation of intercept factor, σ_{eq} is used in step (1) in the place of σ_s of the above procedure.

D. POINTING ERROR

An additional error mechanism which is present in all solar collector systems is the pointing error (δ), which is defined as the angular offset difference between the center of the receiver aperture and the center of the solar flux distribution generated by the concentrator. Included within this category of errors are relatively constant or slowly time varying sources of inaccuracy such as atmospheric refraction and misalignments. Other errors within this class are of a more transient nature and can be originated by wind load deflections and control system hysteresis. Nevertheless, the pointing error must be interpreted as being the instantaneous value, and it may indeed vary with time.

Except in an ideal case, the geometrical center of the receiver aperture does not coincide with the center of the generated solar flux image due to the concentrator pointing error. An illustration of this phenomenon is given in Figure 2-3. Consequently, an increase in pointing error results in a smaller quantity of energy being directed through the receiver aperture. Obviously, the presence of a pointing error then represents lost energy, and it is advantageous to determine the cost effective limits of minimizing this error by such means as more precise sensing, more frequent calibration, and decreasing the mechanical errors in the control system gears and motors.

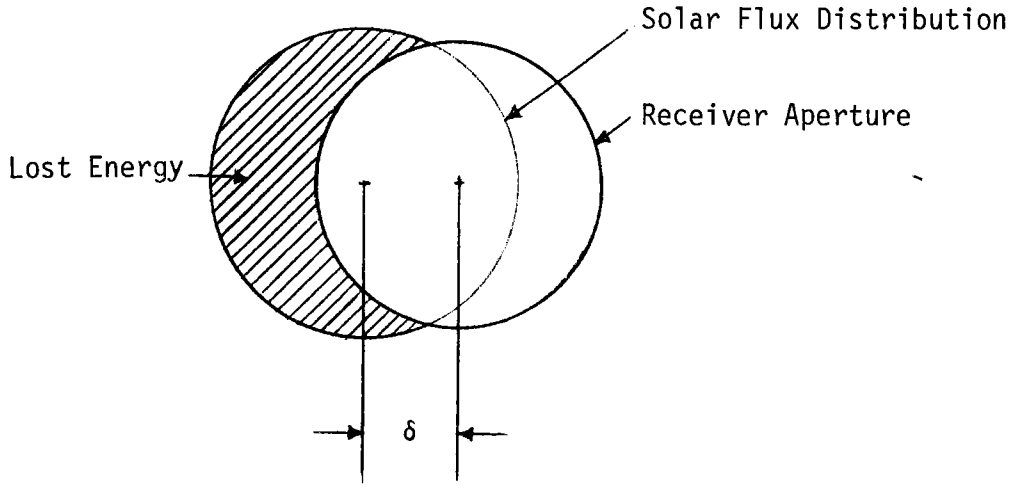

Figure 2-3 Concentrator Pointing Error (δ)

As a result of the previous discussion, it can be seen that pointing or tracking errors are distinct from the class of errors due to optical deficiencies (i.e. slope, contour, and specular errors). The optical errors are responsible for determining the resultant shape of the solar flux distribution at the focal plane of the concentrator, while the pointing error (for values less than approximately 1^{o}) merely varies its locational relationship to the receiver aperture which changes only the intercept factor (ϕ) resulting in reduced efficiency.

Each given control system will have an inherent pointing error behavior and this characteristic will affect only the value of the intercept factor. A rigorous analysis of the pointing error is given by Hughes (Ref. 1 and 2). Using existing control techniques, pointing errors can be made small compared to optical surface errors. Therefore, for the purpose of this analysis which is the computer modeling and optimization of the collector system (concentrator, receiver, heat engine, etc.), the value of the pointing error is assumed to be zero ($\delta = 0$). This is a valid simplification considering that present study goals are not inclusive of the tracking or control scheme to be employed.

E. INTERCEPT FACTOR

The intercept factor (ϕ) is a term quantifying the percentage of concentrated solar energy that actually enters the receiver (Q_{AI}) and is subsequently available for further energy conversion. The accepted value of the intercept factor is a statistical expression that is a function of the long term average pointing errors from the control system (δ), the radius of the receiver aperture (RA), and the standard deviation of the solar flux distribution (σ_G). As was previously described, a principal assumption that was made to simplify the derivation of the intercept factor is that the solar flux distribution which is created by the concentrator reflective surface is Gaussian at the focal plane.

The equation for the intercept factor in consideration of the assumptions given can be expressed as follows:

$$\phi = 1 - e^{-RA^2/2\,\sigma_G^2}, \quad \text{when } \delta \text{ (pointing error)} = 0$$

If the size of the receiver aperture is small in relation to the concentrated flux distribution or if the midpoint of the flux distribution does not coincide with the geometric center of the receiver aperture, then the total quantity of energy entering the aperture will be perceptibly less than the ideal (100 percent). The percentage of energy which is actually captured in the receiver is defined as the intercept factor. Obviously the performance of the receiver is directly related to the intercept factor, and the equation that represents the quantity of energy that enters the receiver from the concentrator can be given as follows:

$$Q_{AI} = (Q_{con}) \quad (\phi)$$

In conclusion, for a selected receiver temperature it should be noted that the intercept factor (ϕ) reflects the effect of complex optics and tracking on the determination of the energy entering the receiver.

SECTION III

RECEIVER CHARACTERIZATION

A. OVERVIEW

The amount of solar thermal energy collected at the cavity receiver and transferred to the transport fluid is significantly influenced by the receiver characteristics. The major parameters of the receiver influencing its efficiency (defined by the ratio of solar energy entering the cavity to the thermal energy transferred to the transport fluid) are: the receiver configuration, aperture diameter, receiver innerwall properties, and receiver insulation. Two receiver configurations were analyzed in this study - conical and cylindrical. The cylindrical receiver is analyzed in greater detail.

B. RECEIVER CONFIGURATIONS

A major portion of heat loss from the receiver is through the aperture opening. In the actual design of the receiver, the receiver configuration is chosen based upon the ease of construction and its ability to achieve the highest possible efficiency for a given aperture diameter.

The conical configuration is simpler from the point of calculating the quantity of reflected radiant energy from the walls escaping through the aperture. However, most of the studies (Garrett (Ref. 4) and others) indicate that a cylindrical configuration is the most suitable from the aspect of receiver construction.

In the case of a cylindrical configuration, the solar flux incident on the cavity walls is affected by the ratio of cylinder height to diameter. For the parabolic dish considered in this study the ratio of dish focal length to dish diameter (f/DC) is 0.6. The cylindrical receiver analyzed in this work has a ratio of 0.5 for its height to diameter. For this dish-receiver configuration, most of the solar flux entering the cavity will be incident only on the bottom wall of the receiver. The heat transfer fluid removes the heat from the receiver by passing through the heat exchanger located near the bottom wall. A schematic of the receiver with the incident solar flux is shown in Figure 3-1.

A change in the value of cylinder height to diameter ratio for a given dish configuration affects the flux distribution on the receiver walls. For ratios smaller than that of the dish (f/DC), all of the solar flux will be incident on a small portion of the bottom wall. Whereas for larger ratios the solar flux will be incident on both the bottom wall and the side wall. One advantage of containing the incident solar flux within the bottom wall is the resulting lower temperatures of the side walls; at lower temperatures the radiation heat loss from the side walls will be smaller.

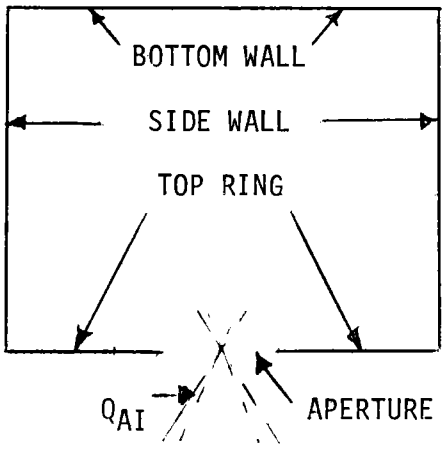

Figure 3-1. Receiver Schematic

C. HEAT LOSSES IN THE RECEIVER

The heat losses in the receiver can be classified into three groups: radiative losses from inner walls through the aperture, radiative and convective heat losses from receiver outer walls, and convective heat loss through the aperture.

1. Radiative Heat Losses Through Cavity Aperture

The radiative heat losses through the aperture from the cavity walls are evaluated from the view factors and radiosities of the walls. For the purpose of evaluating these factors the inner surface of the cavity is divided into three parts - bottom wall, side wall, and top surface around the aperture. Three basic view factors are computed and used for calculating all of the view factors between the three surfaces. The three basic view factors are: between bottom wall and aperture, between bottom wall and aperture plus the top ring, and between side wall and the aperture plus the top ring. The view factors between bottom wall and aperture and between bottom wall and aperture plus the top ring are given by:

$$F_{ba} = 0.5 \left(X_1 - \sqrt{X_1^2 - 4E_1^2 \; D^2}\right)$$

$$F_{bat} = 0.5 \left(X_2 - \sqrt{X_2^2 - 4E_2^2 \; D^2}\right)$$

where:

F_{ba} = view factor from bottom wall to aperture

F_{bat} = view factor from bottom wall to aperture and top ring

X_1 = $\left[1 + (1 + E_1^2)\, D^2\right]$

E_1 = ratio of aperture radius to cavity height, RA/H

D = ratio of cavity height to cavity radius, H/RB

$$X_2 = \left[1 + (1 + E_2^2)\, D^2\right]$$

E_2 = ratio of cavity radius to cavity height

The view factor between side wall and aperture is given by:

$$F_{sa} = 2\, RB^2 \int_0^H \frac{y}{(y^2 + RB^2)^2}\, dy$$

The above three view factors are used (along with the reciprocity law and the relationship that the sum of the view factors for a surface inside the cavity is unity) for evaluating the remaining view factors for the receiver surfaces. An energy balance equation is written for each of the three surfaces in terms of radiosities. The resulting three simultaneous equations in terms of surface radiosities are as follows:

$$(-A_b/\rho_b)\, J_b + (A_s\, F_{sb})\, J_s + (A_t\, F_{tb})\, J_t = A_b\, E_b/\rho_b - Q_{AI}$$

$$(A_b\, F_{bs})\, J_b - (A_s\, (1-F_{ss})/\rho_s)\, J_s + (A_t\, F_{ts})\, J_t = 0$$

$$(A_b\, F_{bt})\, J_b + (A_s\, F_{st})\, J_s - (A_t/\rho_t)\, J_t = 0$$

where:

A_b, A_s, A_t = surface area of bottom, side, and top ring of the cavity

J_b, J_s, J_t = radiosities of three surfaces

ρ_b, ρ_s, ρ_b = reflectance of three surfaces

F_{ij} = view factor from surface i to surface j, b: bottom wall, s: side wall, t: top ring

E_b = emitted energy from the bottom wall, T_b^4

ϵ = emissivity of the walls

Q_{AI} = solar energy entering the cavity

In writing the last two equations, it is assumed that the incident energy, G, on the surface is equal to radiosity, J. This relation approximately holds for cavity walls whose exterior sides are well insulated. The simultaneous equations are solved for radiosities; the radiative heat loss through the aperture is calculated from:

$$Q_{AO} = F_{ba} J_b + F_{sa} J_s$$

2. Radiative and Convective Heat Losses from the Outer Walls

The heat losses from the outer walls of the receiver consist of two parts: convective losses and radiative losses. In Figure 3-2, a circuit analogy of the various heat losses from the receiver walls is shown.

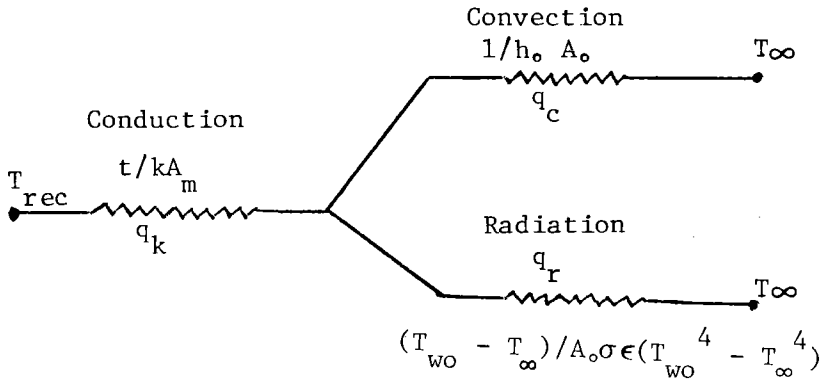

A_o - Rec. outer wall area
Am - Rec. mean wall area
ϵ - Surface emissivity
σ - Boltzmann constant
t - Rec. wall insulation thickness
k - Thermal conductivity of insulation
h_o - Rec. outer wall heat transfer coefficient

Figure 3-2. Receiver Wall Heat Losses

The wall temperature, T_{wo}, is calculated from the equation:

$$q_k = q_c + q_r$$

$$U_k (T_{rec} - T_{wo}) = U_c (T_{wo} - T_\infty) + U_r (T_{wo} - T_\infty).$$

where:

q_k	=	conductive heat loss
q_c	=	convective heat loss
q_r	=	radiative heat loss
U_k, U_c, U_r	=	conductive, convective and radiative heat loss coefficients
T_{rec}	=	receiver bottom wall temperature
T_∞	=	ambient temperature

The radiative and convective heat losses from the wall are given by:

$$Q_l = U_k \ (T_{rec} - T_{wo}).$$

3. Convective Heat Loss Through the Aperture

The convective heat loss through the aperture cannot be easily described in an analytical form. In the present study convective heat loss through the receiver aperture is calculated by using the relation (based on the aperture area, Ref. 5):

$$Q_{LV} = A_{ap} \ h_v \ (T_{rec} - T_\infty)$$

where Q_{LV} is the convective heat loss, A_{ap} the aperture area, and h_v is the convective heat loss coefficient. The convective heat loss coefficient, h_v, is the sum of the natural convective heat transfer coefficient, h_{vn}, and the forced convective heat transfer coefficient, h_{vf}. These convection coefficients are given by the correlations:

$$h_{vn} = 0.0013 \ (T_{rec} - T_\infty)^{1/3}$$

$$h_{vf} = 0.002 \ V$$

where h_{vn} and h_{vf} are in $kW/m^2 \ ^oC$, T_{rec} and T_∞ are in ^oC, and V, the wind velocity (assumed here to be 2m/sec).

The total heat loss from the receiver is the sum of the following: radiative heat loss through the aperture, radiative heat loss from the outer wall, convective heat loss from the outer wall, and convective heat loss through the aperture.

D. OPTIMIZATION FOR APERTURE RADIUS

The amount of solar energy that enters the receiver cavity, for a given dish with a specified slope error, depends on the aperture diameter. In Figure 2-2 it was shown that for smaller aperture openings a lesser amount of solar energy enters the cavity. At the same time it was shown in Section III-C.3 that for larger aperture openings, a greater amount of heat was lost by radiation through the aperture opening. The present computer model is constructed such that an optimization procedure is used for choosing the aperture radius. In this scheme, the aperture radius is reduced in steps, and the receiver performance is evaluated. The receiver efficiency is defined by:

$$\eta_{rec} = \frac{Q_{AI} - Q_{AO} - Q_L - Q_{LV}}{Q_{COL}}$$

where:

Q_{COL}	=	solar energy collected by the dish
Q_{AI}	=	solar energy entering the cavity
Q_{AO}	=	radiative heat loss through the aperture opening
Q_L	=	convective and radiative heat loss from receiver outer surface
Q_{LV}	=	convective heat loss through aperture opening

When the aperture diameter is reduced, both Q_{AI} and Q_{AO} decrease for a given value of Q_{COL}. In the above optimization scheme, the optimum aperture size is that at which the receiver efficiency is the highest.

E. TEMPERATURE DISTRIBUTION IN THE CAVITY

The temperature distribution in the cavity is affected by the receiver configuration along with the cavity surface properties and the aperture size. The manner in which the transport fluid removes the heat from the receiver also affects the temperature distribution in the receiver. For receivers where the heat transfer fluid enters near the cavity aperture opening and exits at the bottom wall, the temperature difference between the surfaces could be as high as 800°F; the highest temperatures will be reached at the bottom wall which is designed as a reradiating surface.

For the receiver used in the present study, all the solar flux entering the cavity is incident on the bottom wall; the heat from the receiver is assumed to be removed from the bottom wall.

For the purpose of evaluating the radiosities of the cavity walls, the bottom wall of the receiver is assumed to be maintained at a constant temperature, T_{rec}. The radiosities and, hence, the wall temperatures are evaluated with this assumption. The manner of heat removal from the receiver considered in this study, makes it differ from those which are generally used in dish-engine systems. However, a preliminary check shows that the results from the present model compare favorably with those of other receivers (Ref. 6). This comparison indicates that the results are not a strong function of cavity design for the range of wall to aperture areas being considered ($A_w/A_o \sim 80$). Therefore, this model provides representive trends within the limits of other design uncertainties.

The receiver wall temperatures are determined from the following relationships:

$$T_s = \sqrt[4]{J_s/\sigma}$$

$$T_t = \sqrt[4]{J_t/\sigma}$$

Depending on the receiver temperature and the ratio of cavity surface area to aperture area, the side wall and the top ring temperatures may be slightly above the receiver bottom wall temperature.

SECTION IV

ENGINE CHARACTERIZATION

A. ENGINE SUBSYSTEM

The conversion of heat to mechanical work in heat engines is accomplished by adding the thermal energy to the working fluid at an elevated pressure confined within the engine and, subsequently, allowing the working fluid to produce mechanical work during a restrained expansion process. Any such heat engine must carry the working fluid through a sequence of thermodynamic states in order to convert thermal energy to useful work.

A heat engine is traditionally described according to the thermodynamic cycle on which it operates. A particular thermodynamic cycle is comprised of the sequence of processes that the working fluid undergoes within the confines of the heat engine. In addition to the thermodynamic cycle of a heat engine, it may also be commonly classified as being either an open-cycle or a closed-cycle machine.

In an open-cycle machine, the working fluid is inducted into the engine from the surroundings. It is passed through the engine, therein absorbing heat and producing work, and is then exhausted to the surroundings. In a closed-cycle machine, the working fluid is completely contained within the machine and is recirculated to repeatedly execute the thermodynamic cycle. The heat addition and rejection processes are usually accomplished via heat exchangers.

This study has concentrated solely on the Brayton cycle engine as the heat engine which would be utilized. The ideal thermodynamic cycle of the Brayton engine consists of:

(1) isentropic compression

(2) constant pressure heat addition (partly regenerative)

(3) isentropic expansion

(4) constant pressure heat rejection (partly regenerative)

Brayton cycle engines may also be configured without thermal regeneration, and they may be used as either closed-cycle or open-cycle machines.

Today, the term "Brayton cycle engine" is virtually synonymous with gas turbine engine. Consequently, hereafter the term Brayton or Brayton engine is used in this report as a shorthand way of referring to a Brayton cycle gas turbine engine. At present, the gas turbine engine is widely used in large commercial aircraft and in many stationary applications, where its ability to run efficiently over only a narrow speed range is not a handicap. The gas turbine engine's

simplicity, high specific power, heat source versatility, and smoothness of power delivery has made it a desirable choice for many applications.

The basic open Brayton engine cycle includes four thermodynamic processes. These are described by the following steps:

(1) Compression of the working fluid from ambient pressure to an elevated pressure

(2) Addition of heat to the working fluid at the constant elevated pressure

(3) Expansion of the working fluid back to ambient pressure, with extraction of useful work, and

(4) Rejection of working fluid at constant pressure to atmosphere

One major distinction between Brayton machines lies in whether they operate on an open-cycle or closed-cycle. In an open-cycle machine, the working fluid is predominantly the ambient medium, i.e. air, which flows through the machine and out. A schematic for such a open-cycle is shown in Figure 4-1.

In a closed-cycle machine, the working fluid is a separate medium, totally confined to the engine and cyclically recirculated through the basic processes. Heat is added to the working fluid through a heat exchanger and the source of heat may be any convenient heat source such as, in this case, solar radiation. Any noncondensible gas, including air, could be used as the working fluid, but good efficiency and high power output dictate that the gas be selected for superior thermodynamic properties; helium and hydrogen are widely used in closed-cycle turbines. Such a closed-cycle Brayton engine is illustrated in Figure 4-2.

For a given pre-expansion gas temperature, high thermal efficiency can be obtained using a more moderate expansion ratio across the turbine, together with effective post-expansion scavenging of residual heat from the turbine exhaust. The scavenged heat energy is returned to the working fluid after compression, through a heat exchanger. This type of configuration is commonly called regenerated. A schematic for a open-cycle regenerated engine is given in Figure 4-3. The ideal regenerated Brayton cycle is shown in Figure 4-4.

B. BRAYTON ENGINE THERMODYNAMICS

The thermodynamic processes of Brayton cycle engines are amenable to convenient mathematical representation. Consequently, the performance of Brayton engines may be adequately estimated via analytical techniques. The utilization of such techniques is usually limited only by the availability of performance data on individual

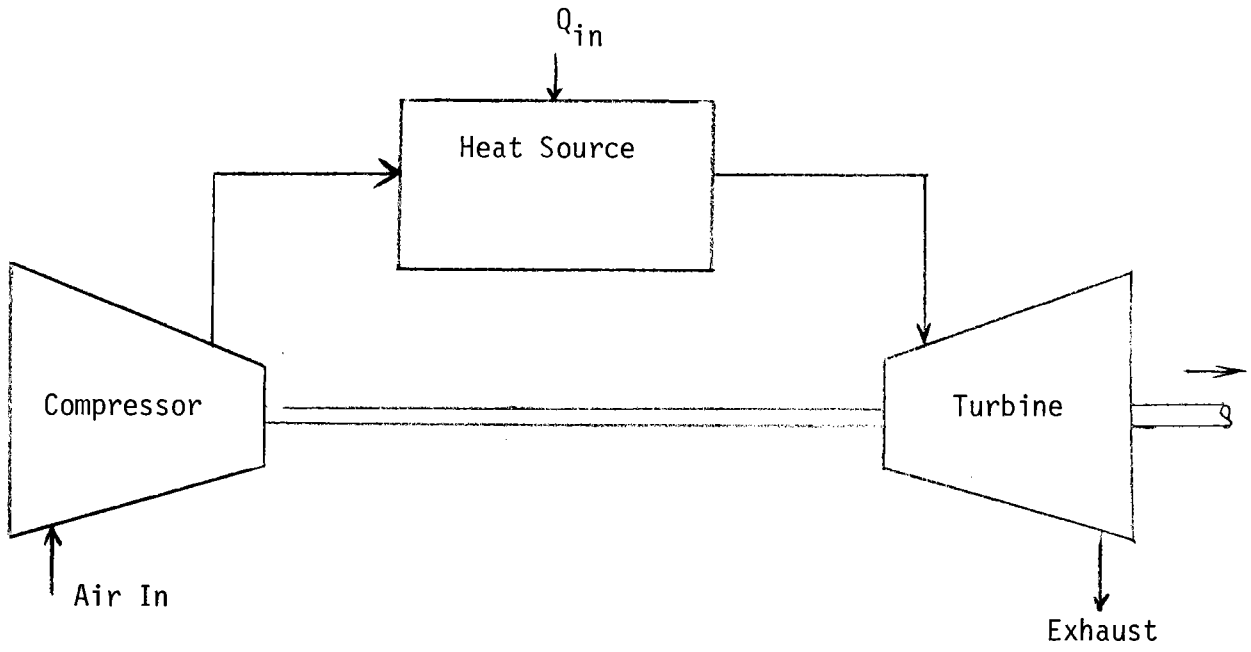

Figure 4-1. Open Cycle Brayton Engine

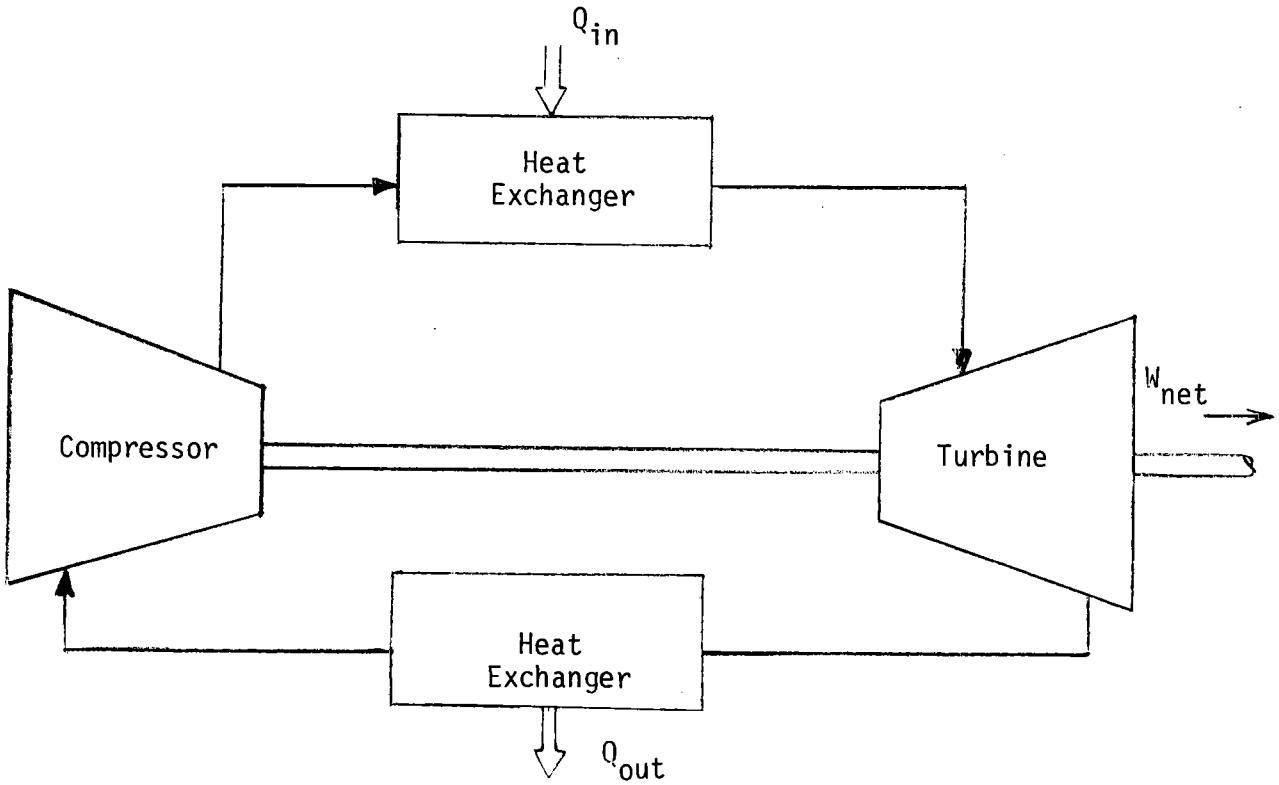

Figure 4-2. Closed Cycle Brayton Engine

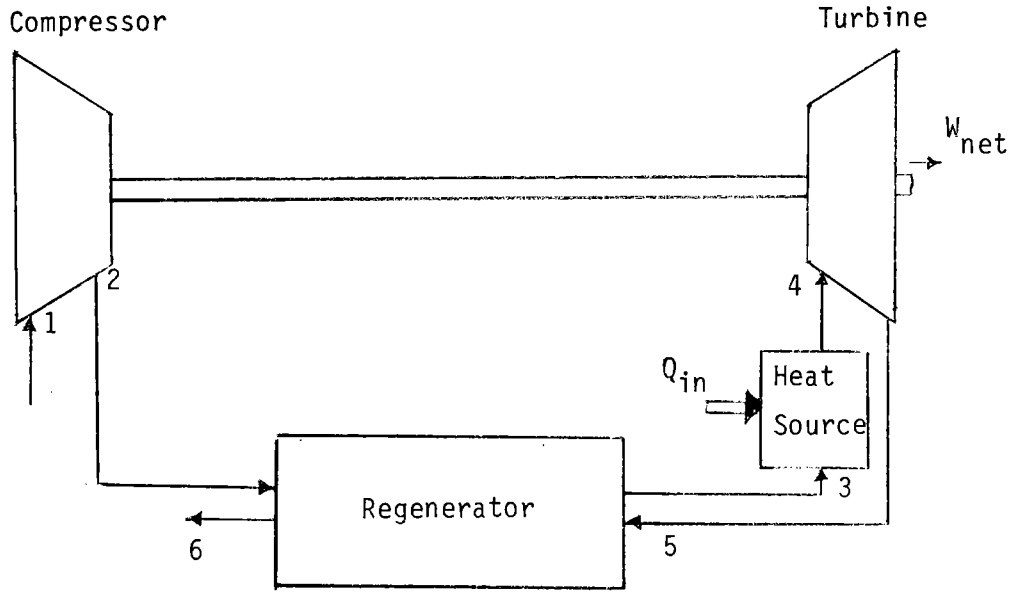

Figure 4-3. Open Cycle Regenerated Brayton Engine

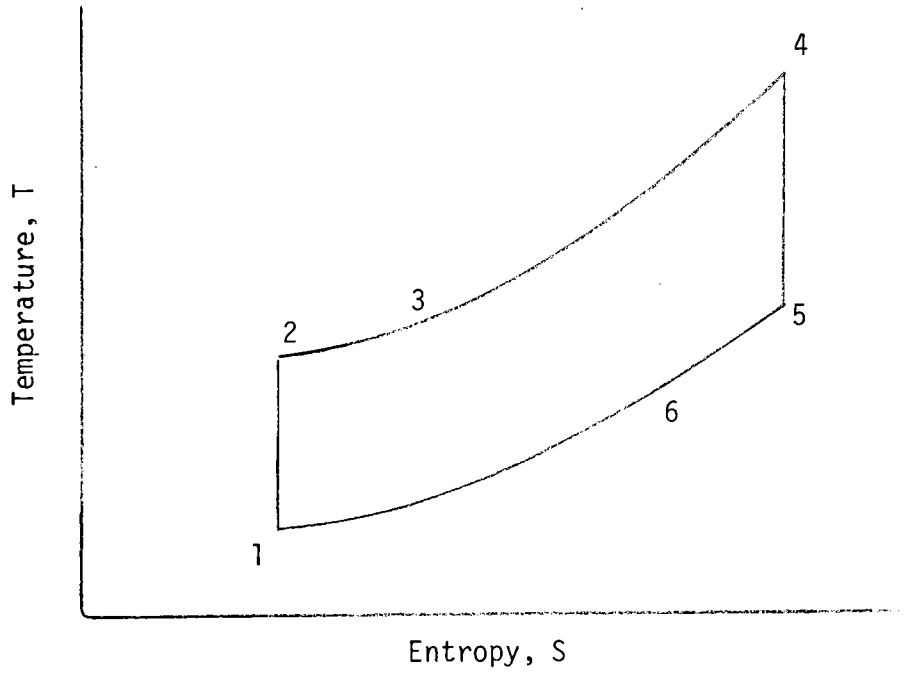

Figure 4-4. Ideal Regenerated Brayton Cycle

components of the engine. The Brayton engine differs fundamentally from the intermittent internal combustion engines in that the processes of compression, heat addition, and expansion occur continuously within the separate and distinct components (Ref. 7). The parameters which describe the performance of the major Brayton engine components -- such as compressors, turbines, and heat exchangers -- are discussed in the next part of this section.

The work output of a Brayton engine may be obtained by algebraically summing the work produced (or absorbed) by the various components of the engine over the prescribed thermodynamic path of the working fluid. Considering the heat addition from the high-temperature source only, in conjunction with the definition of thermal efficiency yields the cycle thermal efficiency, $_{eng}$, as:

$$\eta_{eng} = \frac{w_t + w_c}{q_h}$$

where w_t is the work produced in the expansion process, w_c is the work absorbed in the compression process (a negative quantity), and q_h is the heat added from the high-temperature source.

By taking into account the relations for isentropic changes of state in an ideal gas and the steady flow energy equation, the cycle thermal efficiency may be estimated by computing w_c, w_t, and q_h. The work of compression, w_c, per unit mass of working fluid is given by:

$$w_c = (1/\ _c)\ c_{pa}\ T_{ci}\ (1 - r^{\phi})$$

The turbine work per unit mass of working fluid, W_t, is given by:

$$w_t = \eta_t\ c_{pg}\ T_{ti}\ (1 - (1/(\eta_p r)^{\psi}))$$

The heat input per unit mass of working fluid, q_h, is given by:

$$q_h = c_{pg}\ (T_{ti} - T_{bi})$$

The working fluid temperature at the outlet of the regenerator, T_{bi}, is given by:

$$T_{bi} = T_{co}\ (1 - \epsilon\ ) + \epsilon\ T_{to}$$

The working fluid exit temperatures at the compressor, T_{co}, and turbine T_{to}, are given by:

$$T_{co} = T_{ci}\ (1 - 1/\eta_c + r^{\phi}/\eta_c)$$

$$T_{to} = T_{ti}\ (1 - \eta_t + \eta_t\ (1/(\eta_p r))^{\psi})$$

The turbine inlet temperature, T_{ti}, is related to receiver temperature, T_{rec}, by:

$$T_{ti} = T_{rec} - \Delta T_{rec}$$

where:

r	=	compressor pressure ratio
T_{ci}	=	compressor inlet temperature
T_{ti}	=	turbine inlet temperature
c_{pa}	=	specific heat of air
c_{pg}	=	specific heat of air at elevated temperature
η_c	=	compressor efficiency
λ_a	=	average ratio of specific heats of air during compression
λ_g	=	average ratio of specific heats of air during expansion
η_t	=	turbine efficiency
ϵ	=	regenerator effectiveness
η_p	=	pressure loss factor
ΔT_{rec}	=	temperature drop between receiver and turbine inlet
ϕ	=	$(\lambda_a - 1)/\lambda_a$
ψ	=	$(\lambda_g - 1)/\lambda_g$

The cycle thermal efficiency as predicted by the method described above is subject to the limitations of the basic "lumped parameter" method of describing the performance of the individual engine components and of treating frictional and heat losses. This simplified analysis is considered satisfactory for the establishment of efficiency trends as component performance parameters are changed and for estimating the performance of a Brayton engine at its design point, providing of course that the assumed levels of component performance are attained in practice.

C. COMPRESSOR

Compressor performance at a given operating point, which is defined by mass flow, shaft speed, and pressure ratio, is usually described in terms of the compressor efficiency, η_c, which is the ratio of the isentropic enthalpy increase to the actual enthalpy increase of the working fluid as it passes through the compressor from

inlet pressure to outlet pressure. This definition is for the compression process with no appreciable heat transfer to, or from, the working fluid. By using the above definition of compressor efficiency, the relations for isentropic changes of state of an ideal gas, and the steady-flow energy equation, it is possible to express the compressor work in terms of the independent Brayton engine parameters and the gas constants for the working fluid. The compressor work, w_c, will appear as a negative quantity, indicating that shaft work was absorbed.

The Brayton engine demands high compressor efficiency at pressure ratios ranging from about 2:1 to 5:1. Either positive displacement or aerodynamic compressors can meet this requirement. Since the high pressure ratio capability of the positive displacement compressor is not required, the high air handling capacity of an aerodynamic compressor can be exploited to minimize size and weight for an engine of a specified maximum power. Good design can result in compressor efficiencies of 80% to 85% for a steady-flow aerodynamic compressor at pressure ratios ranging from 3:1 to 6:1 beginning with ambient air.

D. TURBINE

Turbine performance may be described in a manner similar to that of compressor performance. The efficiency of a turbine may be expressed as the ratio of the actual enthalpy decrease to the isentropic enthalpy decrease of the working fluid as it expands through the turbine. This process is essentially an adiabatic one. By using the previous definition of turbine efficiency, the relations for isentropic changes of state of an ideal gas, and the steady-flow energy equation, it is also possible to express the turbine work in terms of independent engine parameters and the gas constants for the working fluid.

The performance requirements for the expander of Brayton engines are similar to those of the compressor, with the additional requirement of continuous operation at elevated temperatures. Considerations of pressure ratio and gas handling capacity of expanders comparable to those for the compressor lead to the selection of aerodynamic turbine expanders. However, the choice between axial-flow and radial-flow turbines is not as clear.

At turbine pressure ratios comparable to those of the compressor, turbine efficiencies range from about 85% to 90%. Fewer data are at hand for positive displacement machines; however, with good design to minimize throttling across valves and mechanical friction, they probably would show comparable efficiencies with a somewhat broader range of operating variables.

E. HEAT EXCHANGER

The effect of post-expansion heat recovery on the thermal efficiency of a Brayton engine may be estimated by using the concept of heat exchanger effectiveness. For this simplified analysis, the effectiveness of the heat exchanger will be taken as:

$$\epsilon = \frac{T_{bi} - T_{co}}{T_{to} - T_{co}}$$

where T_{bi} is the heat source inlet temperature, T_{co} is the compressor exit temperature, and T_{to} is the turbine exhaust temperature.

The value of T_{bi} in a regenerated Brayton engine is determined by the temperature rise during compression and the temperature rise during regeneration . Consequently T_{bi} may be expressed in terms of the parameters which describe the performance of the compressor and the regenerator, and in terms of the temperatures T_{ci} and T_{ti} which are taken as independent variables.

A rotary periodic-flow regenerator suitable for the Brayton engine can be designed for an effectiveness greater than 0.9, with a total pressure loss of less than 10%, and a total leakage of less than 5%. However a primary difficulty in the past with the regenerated Brayton engine has been the availability of a low-cost, high-temperature material for the regenerator. At the present time, aluminum silicate regenerator disks are under development for automobile gas turbine applications. Also other ceramic materials are being tested for turbine rotors and flow path components (Ref 8).

F. BRAYTON ENGINE COMPUTER MODEL

As a result of the previously described thermodynamic cycle analysis of the Brayton engine, it has been possible to formulate a computer model of the engine in terms of the independent engine parameters. The computer model has been developed in such a manner that both open-cycle and closed-cycle configurations can be evaluated. The gas constants for the working fluid of the Brayton engine are also a program input so that various fluids may be investigated in the course of the study. Consequently, it is possible to vary any one of the independent engine parameters while holding the others constant in order to investigate the sensitivity of engine efficiency to the independent parameter in question. Such a sensitivity analysis will provide valuable data to assist in the determination of the most advantageous areas in which to concentrate future research and development activities which would have the greatest potential for engine efficiency improvement.

The engine model developed here is quite flexible; it can evaluate the performance of engines of any given size. To evaluate the performance of an engine of a particular size, the independent engine parameters for that engine are evaluated and input to the model. The input parameters which characterize the size of the engine are: compressor and turbine efficiencies, regenerator effectiveness, and pressure loss factor.

SECTION V

DISH-BRAYTON SYSTEM (DBS) CHARACTERIZATION

A. SYSTEM MODEL

The subsystem models developed in the previous sections are integrated via a computer code to obtain the system model. This computer code is capable of evaluating the performance of the dish-Brayton system. The inputs to this model consists of key component parameters such as geometric configuration of dish receiver and compressor efficiency, and the operating conditions such as receiver temperature, ambient, and turbine inlet temperatures. The basic processes that are evaluated in this model are the following:

(1) Focusing of the ambient insolation into a concentrated solar flux by the parabolic dish

(2) Capturing of this solar flux and conversion into thermal energy by the receiver located at the focus of the dish

(3) Transfer of the above thermal energy to a working fluid in a high temperature heat exchanger

(4) Conversion of this thermal energy into mechanical work in a Brayton engine for generating electricity and,

(5) Recovery from the heat of the exhausting working fluid in a recuperator or regenerator.

Figure 5-1 is a simplified block diagram of the entire system showing the roles of major subsystems. In Figure 5-2, a block diagram of the open-cycle Brayton engine subsystem is shown.

B. COMPUTER MODEL

The computer model is structured such that once the values of the design constants and system input variables have been read into the program, the value for the concentrated solar flux, Q_{con}, is computed according to the method described in of Section II-B. The quantity of the concentrated solar flux which actually enters the receiver, Q_{AI}, through the aperture is computed according to the procedure shown in of Section II-E. The receiver subprogram determines the various heat losses: radiation loss through aperture, Q_{AO}, convective and radiative losses from the receiver outer walls. Based on the net thermal energy received by the cavity, Q_{rec}, the receiver efficiency, η_{rec}, is calculated from the ratio, Q_{rec}/Q_{con}.

In the engine subsystem of the computer model, the compressor work, w_c, and turbine work, w_t, of the Brayton engine are calculated from the engine input variables and the cycle working

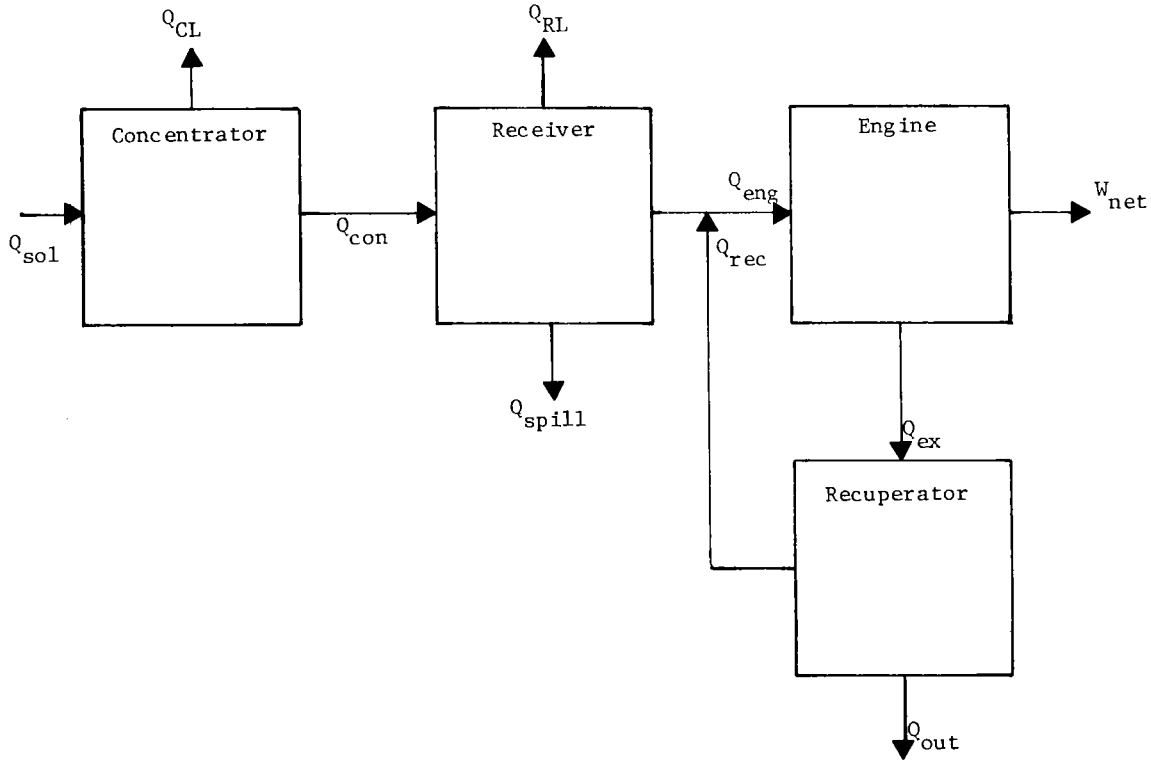

Figure 5-1. System Block Diagram

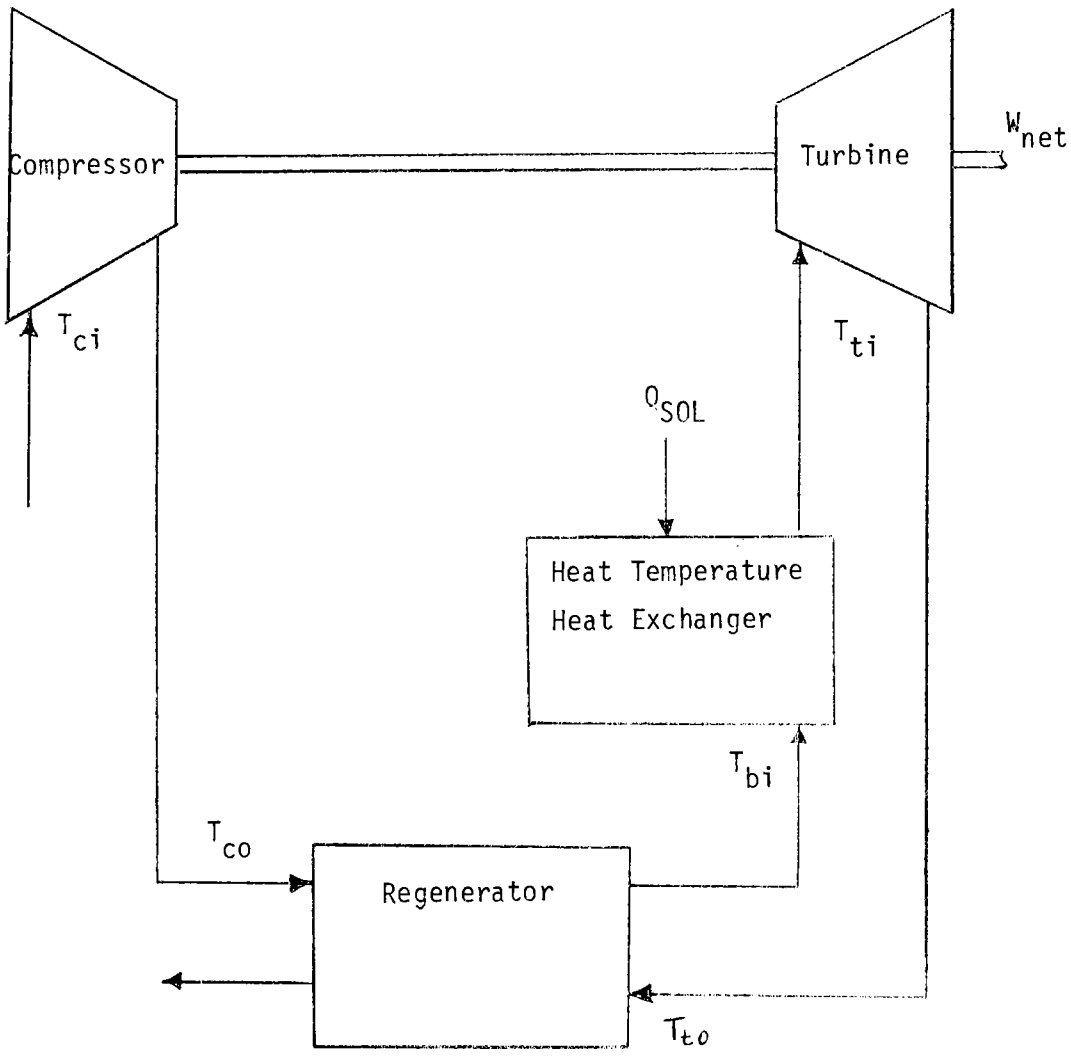

Figure 5-2. Brayton Engine Schematic

fluid state temperatures. The quantity of thermal energy, q_h, available from the heat source to raise the temperature of the working fluid is a function of the cavity temperature and the working fluid properties. The engine efficiency, η_{eng}, is evaluated by the ratio of net engine work output, (w_t-w_c), to the heat added to the engine, q_h. The system efficiency, η_{sys}, for the dish-Brayton system is the product of receiver efficiency, η_{rec}, and the engine efficiency, η_{eng}.

SECTION VI

SUMMARY OF FUTURE WORK WITH DBS MODEL

The dish-Brayton system (DBS) model developed in this study is capable of simulating the performance of the dish-Brayton system at various design conditions. For the purpose of advanced systems identification, it is important that the DBS model has this ability. The DBS model also satisfies the requirement of being able to identify those areas of the system which have greatest potential for system efficiency improvement by performing a sensitivity analysis.

A list of various tasks that are being performed with the DBS model includes the following:

(1) Evaluation of receiver performance at various receiver temperatures

(2) Comparison of DBS model performance with the Garrett Corporation and General Electric Company receiver performance at temperatures of 1500°F and 2500°F

(3) Evaluation of engine performance at various turbine inlet temperatures

(4) Comparison of DBS model performance with that of Garrett Brayton engine

(5) Evaluation of the optimum system (combined receiver and engine) efficiency at various receiver temperatures.

SECTION VII

REFERENCES

1. Hughes, O. R., "Effects of Pointing Errors on Receiver Performance for Parabolic Dish Solar concentrators," 13th IECEC, San Diego, CA, August 20-25, 1978.

2. Hughes, O. R., "Efficiency Degradation Due to Tracking Errors for Point Focusing Solar Collectors," ASME Solar Energy Division, San Francisco, CA, December 10-15, 1978.

3. Poon, P., and Higgins, S., "Optical System of the Advanced Dish-Stirling Module," IOM 353-079-271, Jet Propulsion Laboratory, Pasadena, CA, May 1979.

4. "Air Brayton Solar Receiver," Critical Design Review by AiResearch Manufacturing Company of Arizona (Division of Garrett Corporation) held at Jet Propulsion Laboratory, Pasadena, CA, September 28, 1979.

5. Wu, Y.C., and Wen, L. C., "Solar Receiver Performance in the Temperature Range of 300°C to 1300°C," JPL Internal Document No. 5102-82, Jet Propulsion Labortory, Pasadena, CA, October 1978.

6. "Open Cycle Air Brayton Solar Receiver Phase I - Final Report," prepared for Jet Propulsion Laboratory by AiResearch Manufacturing Company of California (Division of Garrett Corporation), No. 79-15677, February 2, 1979.

7. "Should We Have a New Engine? An Automobile Power System Evaluation," JPL Publication SP 43-17, Volume II, Jet Propulsion Laboratory, Pasadena, CA, 1975.

8. "Advanced Gas Turbine Powertrain System Development Project," Progress Report, presented by Detroit Diesel Allison (AM), at DOE Automotive Technology Development Contractor's Meeting, October 23 - 25, 1979, Dearborn, Michigan.

9. "Low Cost Point Focus Solar Concentrator Final Study Report, Phase I - Preliminary Design," prepared for Jet Propulsion Laboratory by General Electric Company, Contract No. 955210, March 1979.

SECTION I

DESCRIPTION OF THE COMPUTER PROGRAM

A. INTRODUCTION

A computer code was written to evaluate the performance of the dish-Brayton system described in the report. This computer code is based on the models of the receiver and the Brayton cycle developed in the report. The code was written in such a way that the program can be used for evaluating the performance of either the combined receiver-engine system or the individual receiver and engine subsystems. The flow diagrams shown in Figures A-1, A-2, A-3, and A-4 represent the plan for evaluating the performance of the combined receiver-engine system. With a few minor modifications, the program can be separated to be run independently as either receiver program or engine program.

B. MAIN PROGRAM

The basic functions performed in this program are the following:

- Read all the necessary inputs: insolation data, concentrator data, receiver data, engine data, and the receiver temperatures at which the system performance is requested.
- Call the receiver subprogram to evaluate receiver performance at the current receiver temperature.
- Call the engine subprogram to evaluate engine performance at the current receiver temperature.
- Compute the system performance at the current receiver temperature from the component (receiver and engine) performances.
- Repeat the above procedure to cover the range of receiver temperatures input to the program.
- Plot various efficiencies -- receiver, engine, and combined system -- against the receiver temperature.

C. SUBPROGRAM RECX

This subprogram has two subroutines along with the subprogram RECX. The subroutines are: ROM and FN. These subroutines are used in the computation of integrals used in receiver cavity surface view factors. The basic functions performed in this subprogram are the following:

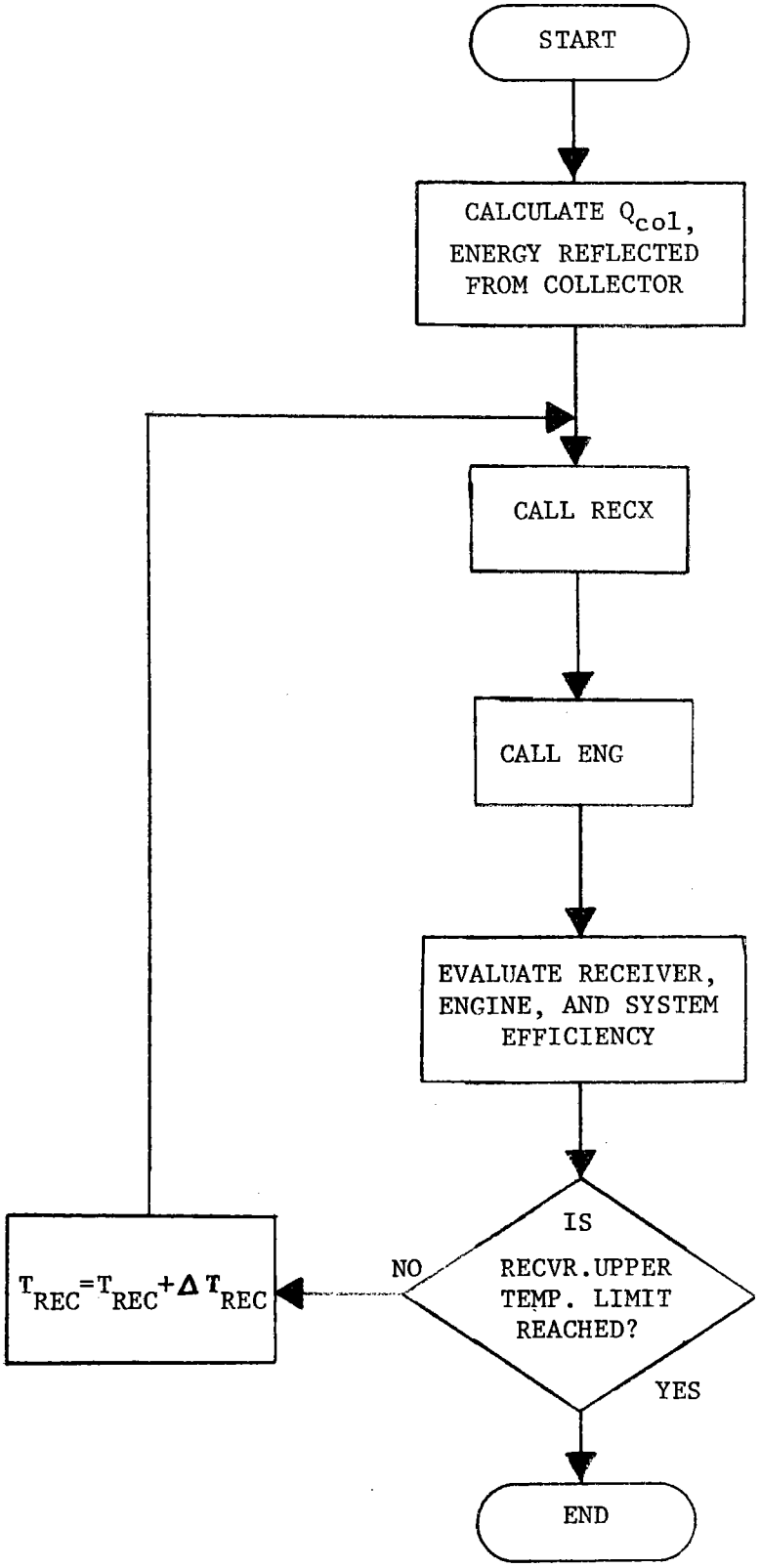

Figure A-1. Flow Diagram of Computer Model

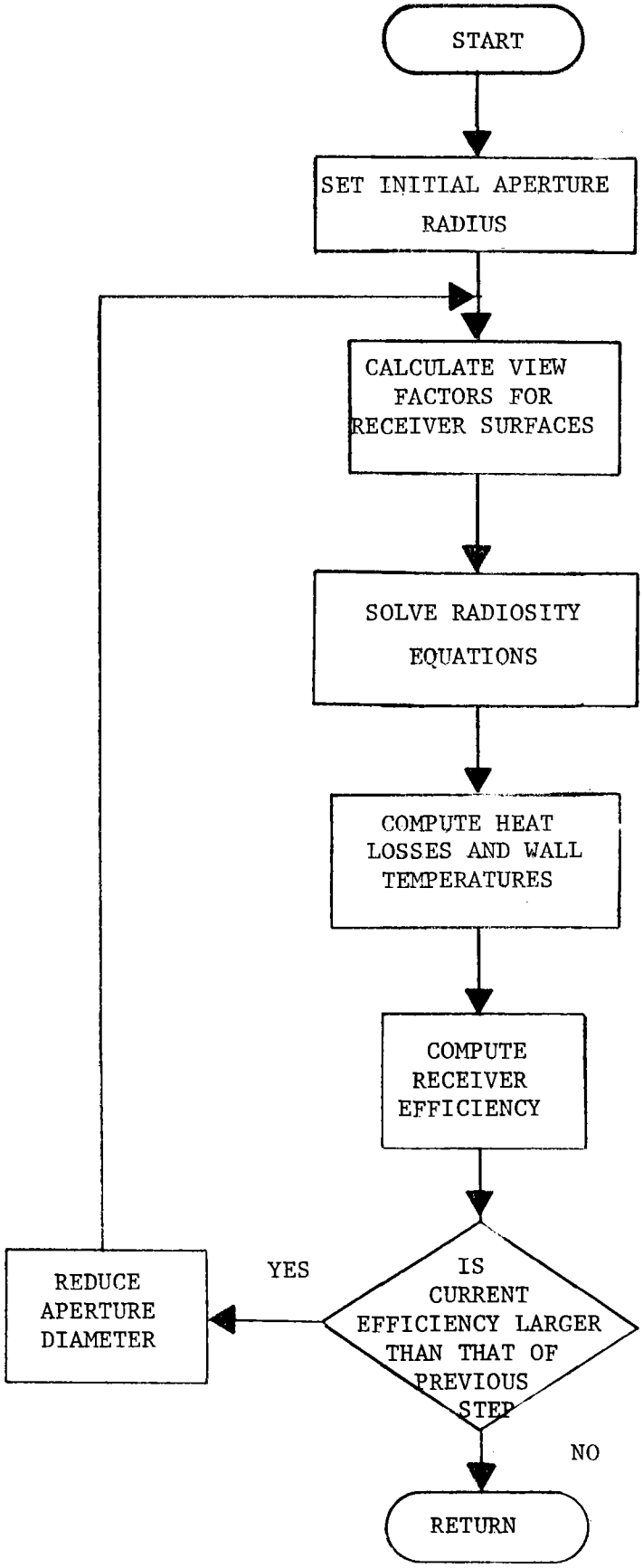

Figure A-2. Flow Diagram of Subprogram RECX

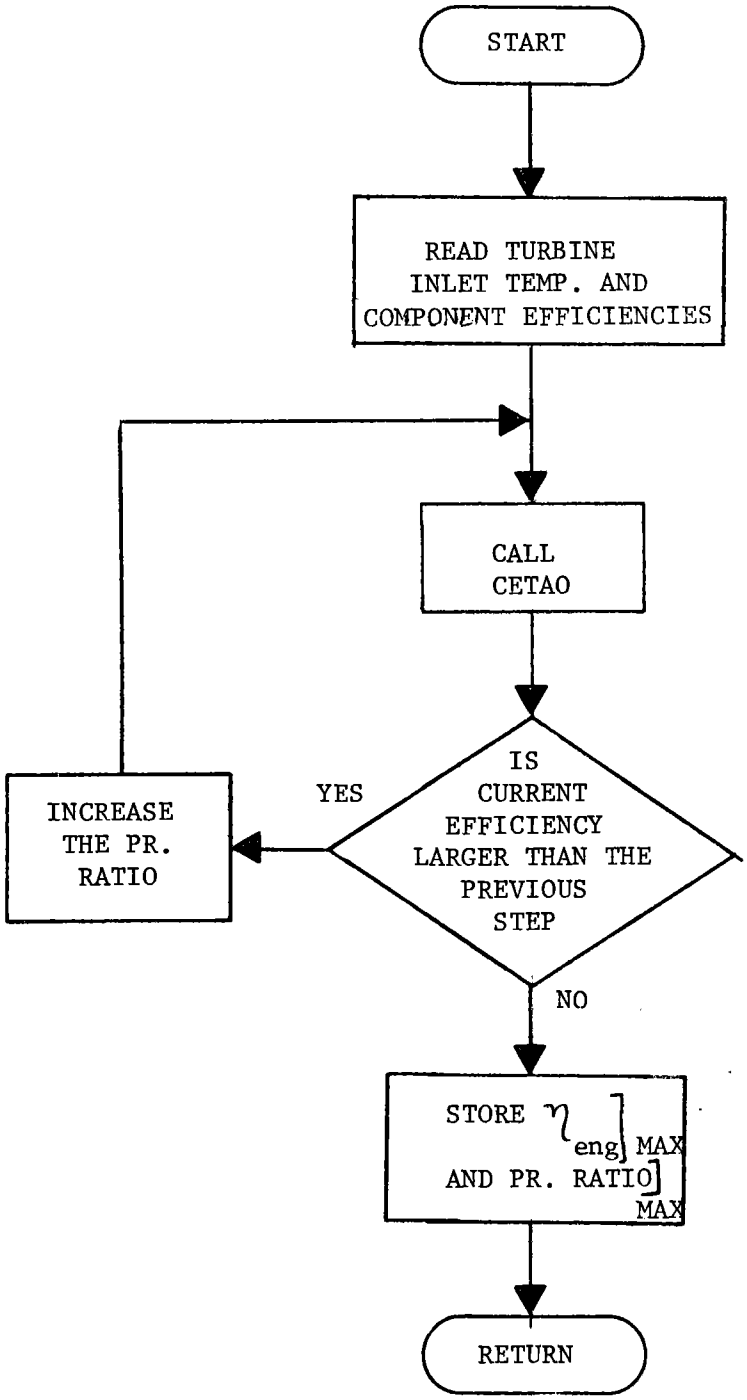

Figure A-3. Flow Diagram of Subprogram ENG

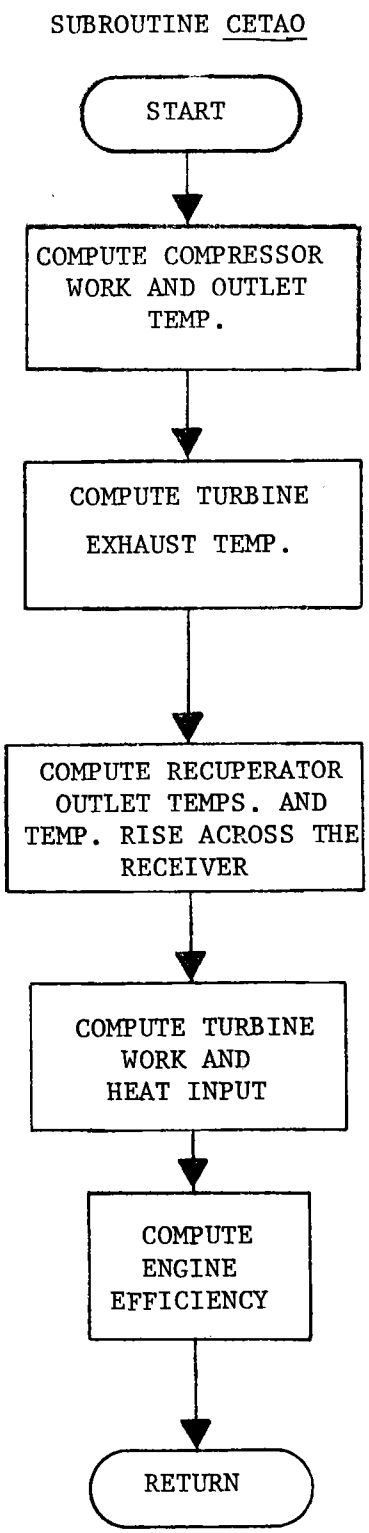

Figure A-4. Flow Diagram of Subprogram CETAO

- o Assuming a large initial value for the aperture radius, compute the aperture intercept factor for the given concentrator surface slope error.

- o For the assumed aperture radius compute the various heat losses from the aperture; compute the receiver efficiency based on these heat losses and the intercept factor.

- o Repeat the above procedure for a decreasing value of aperture radius until a maximum value for the receiver efficiency is obtained.

- o Plot the receiver efficiency against the aperture radius.

D. SUBPROGRAM ENG

This subprogram has two subroutines along with the program ENG. The first one is CETAO which computes the Brayton cycle efficiency. The second is HXH which computes the temperature of air coming out of the receiver before it enters the turbine. The major functions of this subprogram are:

- o For the given receiver temperature, starting with an initial value for the pressure ratio, compute the Brayton cycle efficiency using the component efficiencies.

- o Increase the pressure ratio by the given incremental value and repeat the first step; continue this until a maximum value of efficiency is reached.

E. INPUT TO THE COMPUTER PROGRAM

The input used in this program includes data for the three subsystems: concentrator, receiver, and engine. All the input parameters used are given below.

CPA - Specific heat of air, Btu/lb, ^{o}R

CPU - Specific heat of hot air, Btu/lb, ^{o}R

KA - Ratio of specific heats of air

KG - Ratio of specific heats of hot air

ETAB - Burner efficiency (= 1.0 in the present case)

EFM - Fictitious heat exchange effectiveness between the receiver and the engine, = 1.0 for engine temperature equal to receiver temperature

TCI - Compressor inlet temperature, ^{o}R

ETAC - Compressor adiabatic efficiency

ETAT - Turbine adiabatic efficiency

EPS - Recuperator heat exchange effectiveness

ETAP - Cycle pressure loss factor

TREC - Receiver temperature (up to 25 values), ^{o}R

EL - Recuperator leakage loss factor (= 1.0 in the present case)

TAMB - Ambient temperature, ^{o}R

INS - Solar insolation, W/ft^2

DC - Concentrator diameter, ft

RHOCOL - Concentrator surface reflectivity

RAN - Engine pressure ratio constants
RAN (1) = Starting value of pressure ratio
RAN (2) = Upper limit of pressure ratio
RAN (3) = Incremental value of pressure ratio

IDUMP - Control parameter for printing the results

MRAD - Concentrator surface slope error, milliradians

IREC - Flux intensity at the bottom wall of receiver suns

FOD - Concentrator focal length to diameter ratio, f/DC

EPIS - Receiver surface emissivity,

RHOB - Receiver surface reflectivity,

OIT - Receiver outside insulation thickness, t, ft

KOI - Thermal conductivity of the insulation, $Btu/ft-hr,^{o}F$

HOA - Receiver outer wall convective heat transfer coefficient, $Btu/hr-ft^2$, ^{o}R

SECTION II

LISTING OF THE COMPUTER PROGRAM

The listing of the computer program is given below. In this version of the listing, the subprograms RECX and ENG are combined with the MAIN program. It is necessary to make a few modifications if one wants to run individual subprograms separately. A sample output obtained from this program is listed along with the input data used for the run.

```
AA*PLT(1).DBSM
     1      C      MAIN PROGRAM
     2      C         CPA =AVERAGE SPECIFIC HEAT DURING COMPRESSION
     3      C         CPG =AVERAGE SPECIFIC HEAT DURING EXPANSION
     4      C         KA  =GAS CONSTANT DURING COMPRESSION
     5      C         KG  =GAS CONSTANT DURING EXPANSION
     6      C         ETAB=OVERALL HEAT ADDITION EFFECIENCY
     7      C         PHI =SPECIFIC HEAT RATIO DURING COMPRESSION
     8      C         PSI =SPECIFIC HEAT RATIO DURING EXPANSION
     9      C         ETAP=PRESSURE LOSS FACTOR
    10      C         R   =PRESSURE RATIO
    11      C         DTB =TEMPERATURE RISE ACROSS BURNER
    12      C         TTI =TURBINE INLET TEMPERATURE
    13      C         EPS =HEAT EXCHANGER EFFECTIVENESS
    14      C         TCI =COMPRESSOR INLET TEMPERATURE
    15      C         ETAC=COMPRESSOR EFFICIENCY
    16      C         ETAE=MAXIMUM ENGINE EFFIECIENCY
    17      C         ETAT=TURBIN EFFICIENCY
    18      C         EL  =TOTAL REGENERATOR LEAKAGE
    19              REAL INS
    20              REAL KA,KG,KOI
    21              REAL PI/3.14159/
    22             1REAL RAN(11)/1.,10.,.20,8*0/
    23              REAL TREC(25),ETASYS(25),ETARC(25),ETAEN(25)
    24              COMMON/CONST/CPA,CPG,KA,KG,ETAB,EFH,TCI
    25              COMMON/RECQ/IREC,FOD,EPIS,RHOB,OIT,KOI,HOA
    26              COMMON/DUMP/IDUMP,IPLOT
    27              COMMON/PI/PI,MRAD
    28              COMMON/ENGQ/RP,ETAC,ETAT,EPS,ETAP,EL,RAN
    29      C
    30                NAMELIST/INPUT/CPA,CPG,KA,KG,ETAB,EFH,TCI,RP,ETAC,ETAT,
    31             X  EPS,ETAP,IREC,EL,TAMB,INS,DC,RHOCOL,RAN,IDUMP,
    32             Y  MRAD,IREC,FOD,EPIS,RHOB,OIT,KOI,HOA
    33      C
    34              READ(5,INPUT,END=300)
    35              WRITE(6,INPUT)
    36              CALL  BGNPLT
    37      C
```

```
C
C     COMPUTE THE ENERGY REFLECTED AT THE RECEIVER
C
C
      QCOL=INS*PI/4.*DC**2*RHOCOL
C
C
C     COMPUTE THE RECEIVER,ENGINE, AND THE SYSTEM EFFICIENCIES
C     AT THE INPUT RECEIVER TEMPERATURES
C
C
      IPLOT=3
      DO 500 IT=1,20
      TRI=TREC(IT)
      IF(TRI.EQ.0.)   GO TO 550
      WRITE(6,1410) TREC(IT)
 1410 FORMAT(/////,3X,'RECEIVER TEMPERATURE =',F6.0)
C
C     CALL RECEIVER SUBROUTINE
C
      CALL RECX(QCOL,DC,RHOCOL,TRI,TAMB,QRECM,RAM,ETARCM)
      WRITE(6,1400) ETARCM,RAM,QRECM
1400  FORMAT(//3X,' SUBROUTINE RECEIVER OUTPUT : '//
     X 3X,' ETARCM =',E14.8,3X,'  RAM =',E14.8,3X,' QRECM =',E14.8/)
C
C     CALL ENGINE SUBROUTINE
C
      CALL ENG(TRI,TAMB,ETAEM,RPCM,WNEM)
      WRITE(6,1500) ETAEM,RPCM,WNEM
1500  FORMAT(/3X,' SUBROUTINE ENGINE OUTPUT :'//
     X 3X,' ETAEM =',E14.8,3X,'  RPCM =',E14.8,
     X  '    WNEM =',E14.8/)
C
C     COMPUTE THE SYSTEM EFF AND STORE THE ENGINE,RECEIVER
C     AND SYSTEM EFFS
C
      ETASYS(IT)=ETARCM*ETAEM
      ETARC(IT)=ETARCM
      ETAEN(IT)=ETAEM
      WRITE(6,1600) TREC(IT),ETASYS(IT)
1600  FORMAT(3X,' SYSTEM OUTPUT:',//,3X,' TREC  =',E14.8,6X,'ETASY =
     X,E14.8)
500   CONTINUE
550   CONTINUE
      IT=IT-1
      IF(IPLOT.EQ.3) GO TO 600
C
```

```
C     PLOT EFFICIENCIES VS TEMPERATURE
C
      CALL PLFORM('LINLIN',6.,6.)
      CALL PLSCAL(TREC,IT,2,ETASYS,IT,2)
      CALL PLABEL(' ',1,'TREC',4,'ETASYS',6)
      CALL PLGRAF
      CALL PLCURV(TREC,ETASYS,IT,0,0)
      CALL ADVPLT
      CALL PLFORM('LINLIN',6.,6.)
      CALL PLSCAL(TREC,IT,2,ETARC,IT,2)
      CALL PLABEL(' ',1,'TREC',4,'ETAREC',6)
      CALL PLGRAF
      CALL PLCURV(TREC,ETARC,IT,0,0)
      CALL ADVPLT
      CALL PLFORM('LINLIN',6.,6.)
      CALL PLSCAL(TREC,IT,2,ETAEN,IT,2)
      CALL PLABEL(' ',1,'TREC',4,'ETAENG',6)
       CALL PLGRAF
      CALL PLCURV(TREC,ETAEN,IT,0,0)
600   WRITE(6,2000)
 2000 FORMAT(///'  *** END OF RUN ***')
C
300   CALL ENDPLT
      STOP
         END
```

```
C RECEIVER SUBPROGRAM
C
C     RECEIVER SUBROUTINE
C
      SUBROUTINE RECX (QCOL,DC,RHOCOL,TREC,TAMB,QREC,RAM,ETARCH)
C
      REAL ETARC(200),RAD(200)
      COMMON/FUNCT/YX
      COMMON/PI/PI,MRAD
      DOUBLE PRECISION DARG
      REAL KOI
      DATA SIGMA/0.0033804/
C
C     DATA FOR RECEIVER DIMENSIONS
C
      REAL DT(10,1)
      COMMON/RECQ/IREC,FOD,CPIS,RHOB,OIT,KOI,HOA
      DATA HST/.1/,HMIN/.1E-4/,HMAX/1./
      DATA YY/0./,EPS/1.E-8/,MXSTEP/50000/
      DATA DY/1./
      REAL WORK(20),A(3,3),B(3,1)
```

```
      C
            TP=0.
            SBC=0.1713E-8
            PHE=0.
            QCA=0.
            QA0=0.
            QK=0.
            IDUMP=2
            IPLOT=2
      C
      C     SELECT SIGMA FOR THE GIVEN CONCENTRATOR SLOPE ERROR
      C
            IF(MRAD.EQ.2)SIGMA=.0033804
            IF(MRAD.EQ.3)SIGMA=.004667
            IF(MRAD.EQ.2)ACON=.9991
            IF(MRAD.EQ.3)ACON=.9968
      C
      C     COMPUTE THE RECEIVER DIMENSIONS
      C
            DB=DC/SQRT(IREC)*SQRT(RHOCOL)
            H=FOD*DB
            RB=DB/2.
            D=H/RB
            AB=PI*RB**2
            AS=PI*DB*H
      C
      C     SELECT THE INITIAL VALUE OF APERTURE RADIUS TO BE 1/3 OF
      C     CAVITY RADIUS
      C
       9    CONTINUE
            RA=RB/3.-.016404
            XF=2.*H/DB
            I=1
            NI=0
      C
      C     START COMPUTING THE PERFORMANCE OF THE RECEIVER
      C
      10    CONTINUE
            AA=PI*RA**2
            AT=AB-AA
            DARG=(RA/DC)**2/2./SIGMA**2
            QA0M1=QA0
            QCAM1=QCA
            QKM1=QK
            PHET=PHE
            PHE=ACON*(1.0-1./DEXP(DARG))
            QAI=QCOL*PHE
            E1=RA/H
            X1=1.+(1.+E1*E1)*D**2
            FBA=0.5*(X1-SQRT(X1**2-4.*E1**2*D**2))
            E2=RB/H
            X2=1.+(1.+E2**2)*D**2
```

```
      FBAT=0.5*(X2-SQRT(X2**2-4.*E2**2*D**2))
      FBT=FBAT-FBA
      FBS=1.-FBAT
      FSB=AB/AS*FBS
C
C     COMPUTE FSA USING NUMERICAL INTEGRATION.
C
      EP=EPS
      II=0
      X=0.
      YY=0.
      DST=.1
      DMIN=.1E-4
      KSTEP=0
      YX=2.*RA/DB
C*************************************************************
      CALL ROM(0.,XF,YY)
      FSA=2.*PI*(DB/2.)**2*YY/AS
      FST=FSB-FSA
      FSS=1-FSA-FST-FSB
C
C     SOLVE MATRIX RELATION
C
      A(1,1)=-AB/RHOB
      A(2,2)=-AS*(1-FSS)
      A(3,3)=-AT
      A(1,2)=AS*FSB
      A(1,3)=AB*FBT
      A(2,3)=AS*FST
      A(2,1)=A(1,2)
      A(3,1)=A(1,3)
      A(3,2)=A(2,3)
      EBR=0.1713E-8*TREC**4
      B(1,1)=-(AB/RHOB*EBR*EPS*.2931+QA)
      B(2,1)=0.
      B(3,1)=0.
      CALL SOR(A,3,3,0,3,1,$500,WORK)
      IF (IDUMP.EQ.1) WRITE(6,250)
250   FORMAT(//' MATRIX A AND OUPUT MATRIX B')
      IF(IDUMP.EQ.1) WRITE(6,255) A,B
255   FORMAT(4X,8E15.8)
C
C     COMPUTE APERTURE RADIATION LOSSES USING SURFACE
C     VIEW FACTORS
C
      QA0=AB*FBA*B(1,1)+AS*FSA*B(2,1)
C
C     COMPUTE SURFACE TEMPERATURES
C
      TSIDE=((B(2,1)*3.413)/0.1713E-8)**.25
      TTOP=((B(3,1)*3.413)/0.1713E-8)**.25
      G=QAI/AB
```

```
      C
      C     COMPUTE RECEIVER OUTER SURFACE DIMENSIONS
      C
            ARI=AR+AS+AT
            HO=H+2.*DIT
            CO=PI*(DR+2.*DIT)
            ASO=CO*HO
            ARO=PI*(RB+DIT)**2
            ATO=ARO-AA
            ARO=ABO+ASO+ATO
            ARM=(ARO+ARI)/2
            UK=KOI*ARM/DIT
            UC=HOA*ARO
            NTN=1
            TWOG=TAMB
  310       TWOC=TWOG+1
            NTN=NTN+1
  311       UR=ARO*EPS*(SBC*TWOC**4-SOC*TAMB**4)/(TWOC-TAMB)
            TWOC=(TREC*UK+TAMB*(UC+UR))/(UK+UC+UR)
            DTWO=TWOG-TWOC
            IF(NTN.GT.250) GO TO 312
            IF(ABS(DTWO).GT.1)GO TO 310
  312       TWO=TWOC
      C
      C     COMPUTE THE CONDUCTION LOSSES OF THE RECEIVER
      C
            QK=0.2931*UK*(TREC-TWO)
            QC=0.2931*UC*(TWO-TAMB)
            QR=0.2931*UR*(TWO-TAMB)
      C
      C     APERTURE CONVECTIVE LOSSES
      C
            UCA=0.004+0.0013*((TREC-TAMB)/1.8)**.33
            QCA=UCA*PI*RA**2./3.15*(TREC-TAMB)/1.8*1000.
            QL=QC+QR
            QRECO=QREC
            QREC=QAI-QAO-QL-QCA
      C
      C     RECEIVER EFF
      C
            CTARC(I)=QREC/QCOL
            RAD(I)=RA
            ID=I-1
      C
      C     CHECK WHETHER RECEIVER HAS REACHED MAX EFF AT THIS APERTURE
      C     RADIUS
      C
            IF(I.GT.1.AND.NI.LT.1.AND.CTARC(I).LT.CTARC(ID)) GO TO 205
            RA=RA-0.016404
            IF(RA.LT.0.) GO TO 210
            I=I+1
```

```
177           GO TO 10
178     205   CONTINUE
179           NI=NI+1
180     C
181     C     STORE THE VALUE OF MAX EFF AND THE CORRESPONDING APERTURE
182     C     RADIUS
183     C
184           ETARCM=ETARC(IB)
185           QRECM=QRECB
186           RAM=RAD(IB)
187     210   CONTINUE
188           GO TO 230
189     100   FORMAT(3(2X,8E15.8/))
190     C
191     C     PLOT OF RECEIVER EFF VS APERTURE RADIUS
192     C
193           CALL PLFORM('LINLIN',6.,6.)
194           CALL PLSCAL(RAD,I,2,ETARC,I,2)
195           CALL PLABEL (' ',1,'RA ',5,' ETARC ',8)
196           CALL PLGRAF
197           CALL PLCURV(RAD,ETARC,I,0,0)
198           CALL ADVPLT
199     500   WRITE(6,220)
200     220   FORMAT('A MATRIX IS SINGULAR ,RUN ABORTED')
201     230   CONTINUE
202           RETURN
203           END
```

```
1       C   ENGINE SUBPROGRAM
2       C
3       C
4       C
5       C         CPA =AVERAGE SPECIFIC HEAT DURING COMPRESSION
6       C         CPG =AVERAGE SPECIFIC HEAT DURING EXPANSION
7       C         KA  =GAS CONSTANT DURING COMPRESSION
8       C         KG  =GAS CONSTANT DURING EXPANSION
9       C         ETAB=OVERALL HEAT ADDITION EFFECIENCY
10      C         PHI =SPECIFIC HEAT RATIO DURING COMPRESSION
11      C         PSI =SPECIFIC HEAT RATIO DURING EXPANSION
12      C         ETAP=PRESSURE LOSS FACTOR
13      C         R   =PRESSURE RATIO
14      C         DTB =TEMPERATURE RISE ACROSS BURNER
15      C         TTI =TURBINE INLET TEMPERATURE
16      C         EPS =HEAT EXCHANGER EFFECTIVENESS
17      C         TCI =COMPRESSOR INLET TEMPERATURE
18      C         ETAC=COMPRESSOR EFFICIENCY
19      C         ETAT=TURBINE EFFICIENCY
20      C         EL  =TOTAL REGENERATOR LEAKAGE
21      C         EFR =HEAT EXCHANGE EFFECTIVENESS BET. REC. AND
22      C              ENGINE, =1 FOR ENG. TEMP. EQUAL TO REC. TEMP.
```

```
      C
      C
            SUBROUTINE ENG(TREC,TAMB,ETAEM,RPCM,WNEM)
            REAL KA,KG
            REAL GRX(100),GRY(100),WNE(100),YLIM(3)
            REAL RAN(11)
            COMMON/ENGQ/RP,ETAC,ETAT,EPS,ETAP,EL,RAN
            COMMON/CONST/CPA,CPG,KA,KG,ETAB,EFH,TCI
            INTEGER YN(10)/3*' ',' CYCLE EFFICIENCY',4*' '/
           0INTEGER XN(14)/
           14*' ','   COMPRESSOR PRESSURE RATIO  ',5*' '/
            INTEGER TI(14)/2*' ',' OVERALL CYCLE EFFICIENCY VS',7*' '/
      9     CONTINUE
            IDUMP=2
            IPLOT=1
            IF(IDUMP.EQ.1) WRITE(6,500) CPA,CPG,KA,KG,ETAB,EFH
            IF(IDUMP.EQ.1) WRITE(6,500) RAN
            IF(IDUMP.EQ.1) WRITE(6,500) RP,ETAC,ETAT,EPS,ETAP,TRI,
           XEL,TCI
      500   FORMAT(4X,6E14.8)
      C
      C      SPECIFIC HEAT RATIOS
      C
            PSI=(KA-1.)/KA
            PHI=(KG-1.)/KG
            YMAX=1.E-6
            YMIN=1.E+6
            RP=RAN(1)
            RPI=RP
            FI=RAN(2)
            DE=RAN(3)
            NP=1
      C
      C
      C     EVALUATE THE CYCLE EFFICIENCY AT VARIOUS PR. RATIOS
      C
      C
      C
      C     CALL SUBROUTINE CETA0 TO CALCULATE CYCLE EFF.
      C
        150 ST=RAN(1)
            DO 200 I=1,100
            RP=ST
            CALL CETA0(TREC,TAMB,GRY(NP),TTI,TCI)
            GRX(NP)=ST
            YMAX=AMAX1(GRY(NP),YMAX)
            YMIN=AMIN1(GRY(NP),YMIN)
            NP=NP+1
            ST=ST+DE
            IF(ST.GT.FI) GO TO 210
        200 CONTINUE
        210 NN=NP-1
            RP=RPI
```

```
      C
      C     LOCATE THE PR. RATIO AT WHICH EFF. IS MAX.
      C
            DO 220 I=1,NN
            IF(GRY(I).NE.YMAX)  GO TO 220
            IMAX=I
      220   CONTINUE
      C
      C     STORE THE VALUES OF  EFF., SHAFT OUTPUT, AND PR. RATIO
      C     AT PR. RATIO WHERE EFF. IS MAXIMUM
      C
      C
            ETAEM=YMAX
            WNEM=WNE(IMAX)
            RPCM=GRX(IMAX)
      C
      C     PRINT THE VALUES OF MAX. EFF., MAX. WORK, AND THE PR. RATIO

      C
            IF(IDUMP.EQ.1)
           XWRITE(6,255)TREC,RPCM,ETAEM,ETAC,ETAT,EPS,ETAP
       255  FORMAT(10X,'TREC,RPCM,ETAEM',7F8.3)
            GO TO 299
            IF(IPLOT.NE.1) RETURN
      C
      C     SELECT SCALES FOR PLOTTING EFF. VS PR. RATIOS
      C
            YLIM(1)=YMIN
            YLIM(2)=(YMAX-YMIN)/2.+YMIN
            YLIM(3)=YMAX
            CALL PLFORM('LINLIN',6.,6.)
            DO 230 I=5,10
      230   TI(I+3)=XN(I)
            IF (IDUMP.EQ.1) WRITE(6,1050) TI
      1050  FORMAT(14A6)
            CALL PLSCAL(GRX,NN,2,YLIM,3,2)
            CALL PLABEL(TI(3),72,XN(5),60,YN,60)
            CALL PLGRAF
            CALL PLCURV(GRX,GRY,NN,0,0)
            IF (IDUMP.EQ.1) WRITE(6,1200) (GRX(I0),GRY(I0),I0=1,NN)
      1200  FORMAT(/3X,8E14.8)
            WRITE(6,1300)
      1300  FORMAT(//)
      225   CONTINUE
       299  CONTINUE
            CALL ENDPLT
            RETURN
      C
      C
            SUBROUTINE CETA0(TREC,TAMB,ETAE,TTI,TCI)
            Z1=(1/(ETAP*RP))**PHI
            Z2=RP**PSI
            TR0=0.
            TC0=TCI*(1.-1./ETAC+Z2/ETAC)
            WC=1/ETAC*CPA*TCI*(1-Z2)
```

```
      TTI=TREC
111   TT0=TTI*(1.-ETAT+ETAT*Z1)
      TBI=TC0*(1.-EPS)+EPS*TT0
      TTIL=TTI
      CALL HXH(TBI,TREC,TTI)
      TTEST=TTIL-TTI
      IF(ABS(TTEST).GT.1.) GO TO 111
      DTB=TTI-TBI
      WT=EL*ETAT*CPG*TTI*(1-Z1)
      WNE(I)=WT+WC
      QR=(EL*CPG*DTB)
      QH=QB/ETAB
      ETAE=WNE(I)/QH
      IF(ETAE.LT.0.) ETAE=0.
      RETURN
C
C
      SUBROUTINE HXH(TBI,TREC,TTI)
      TTI=TBI*(1. EFH)+EFH*TREC
      RETURN
C
      END
```

```
      SUBROUTINE ROM(A,B,ANS)
       DIMENSION Q(10,10)
C     ROMBERG TYPE INTEGRATION
      M=10
      Q(1,1)=((B-A)/2.0)*(FN(A)+FN(B))
      MM1=M-1
      DO 1 K=1,MM1
      Q(1,K+1) = Q(1,K)/2.0
      LM=2**(K-1)
      DO 2 J=1,LM
      X=A+(1.0+2.0*(J-1.0))*(B-A)/2.0**K
      VALUE =FN(X)*(B-A)/2.0**K
 2    Q(1,K+1)  = Q(1,K+1) + VALUE
 1    CONTINUE
      DO 3 N=2,M
      MN1=M-N+1
      DO 4 L=1,MN1
 4     Q(N,L)=((4.0**(N-1))*Q(N-1,L+1)-
     1Q(N-1,L))/(4.0**(N-1)-1.0)
 3    CONTINUE
      ANS=Q(M,1)
      RETURN
      END
```

```
        FUNCTION FN(X)
C FUNCTION FOR RECX32
       COMMON/FUNCT/YX
        FSQR=(X**2+YX**2+1.)
        FN=X/2.*(FSQR/SQRT(FSQR**2-4.*YX**2)-1.)
       RETURN
        END
```

```
1       $INPUT CPA=.24,CPG=.285,KA=1.4,KG=1.32,ETAB=1.0,EFH=1.0,TCI=545.,

2       ETAC=.80,ETAT=.87,EPS=.93,ETAP=.92,TREC=1460.,1560.,1660.,
3       1760.,1860.,1960.,EL=1.0,TAMB=545.,INS=74.32,DC=32.808,RHOCOL=.8,

4       RAN=1.,10.,.20,IDUMP=2,MRAD=2,TREC=100,FOD=.6,EPIS=.9,
5       RHOB=.1,OIT=.4,KOI=.03,HOA=1.
6       $END
```

```
$INPUT
CPA     =     .24000000E+00
CPG     =     .28500000E+00
KA      =     .14000000E+01
KG      =     .13200000E+01
ETAB    =     .10000000E+01
EFH     =     .10000000E+01
TCI     =     .54500000E+03
RP      =     .00000000E+00
ETAC    =     .80000000E+00
ETAT    =     .87000000E+00
EPS     =     .93000000E+00
ETAP    =     .92000000E+00
TREC    =     .14600000E+04,   .15600000E+04,   .16600000E+04,   .17600000E+04,

              .18600000E+04,   .19600000E+04,   .00000000E+00,   .00000000E+00,

              .00000000E+00,   .00000000E+00,   .00000000E+00,   .00000000E+00,

              .00000000E+00,   .00000000E+00,   .00000000E+00,   .00000000E+00,

              .00000000E+00,   .00000000E+00,   .00000000E+00,   .00000000E+00,

              .00000000E+00,   .00000000E+00,   .00000000E+00,   .00000000E+00,

              .00000000E+00
EL      =     .10000000E+01
TAMB    =     .54500000E+03
INS     =     .74320000E+02
DC      =     .32808000E+02
RHOCOL  =     .80000000E+00
RAN     =     .10000000E+01,   .10000000E+02,   .20000000E+00,   .00000000E+00,

              .00000000E+00,   .00000000E+00,   .00000000E+00,   .00000000E+00,

              .00000000E+00,   .00000000E+00,   .00000000E+00
```

```
IDUMP   =                +2
MRAD    =                +2
IREC    =              +100
FOD     =      .60000000E+00
EPIS    =      .90000000E+00
RHOB    =      .10000000E+00
OIT     =      .40000000E+00
KOI     =      .30000000E-01
HOA     =      .10000000E+01
$END
```

RECEIVER TEMPERATURE = 1460.

SUBROUTINE RECEIVER OUTPUT :

ETARCM = .93741128+00 RAM = .34143679+00 QRECM = .47044907+05

SUBROUTINE ENGINE OUTPUT :

ETAEM = .22988188+00 RPCM = .21999999+01 WNEM = .15566778+02

SYSTEM OUTPUT:

TREC = .14600000+04 ETASY = .21549387+00

RECEIVER TEMPERATURE = 1560.

SUBROUTINE RECEIVER OUTPUT :

ETARCM = .92867973+00 RAM = .34143679+00 QRECM = .46638440+05

SUBROUTINE ENGINE OUTPUT :

ETAEM = .26645065+00 RPCM = .23999999+01 WNEM = .21112123+02

SYSTEM OUTPUT:

TREC = .15600000+04 ETASY = .24744732+00

RECEIVER TEMPERATURE = 1660.

SUBROUTINE RECEIVER OUTPUT :

ETARCM = .91884753+00 RAM = .34143679+00 QRECM = .46181690+05

SUBROUTINE ENGINE OUTPUT :

ETAEM = .29843490+00 RPCM = .2399999+01 WNEM = .25444071+02

SYSTEM OUTPUT:

TREC = .16600000+04 ETASY = .27421617+00

RECEIVER TEMPERATURE = 1760.

SUBROUTINE RECEIVER OUTPUT :

ETARCM = .90860514+00 RAM = .32503279+00 QRECM = .4558268+05

SUBROUTINE ENGINE OUTPUT :

ETAEM = .32710490+00 RPCM = .2599999+01 WNEM = .31839982+02

SYSTEM OUTPUT:

TREC = .17600000+04 ETASY = .29728195+00

RECEIVER TEMPERATURE = 1860.

SUBROUTINE RECEIVER OUTPUT :

ETARCM = .89715967+00 RAM = .32503279+00 QRECM = .4505454+05

SUBROUTINE ENGINE OUTPUT :

ETAEM = .35263410+00 RPCM = .2799999+01 WNEM = .38614702+02

SYSTEM OUTPUT:

TREC = .18600000+04 ETASY = .31636909+00

```
RECEIVER TEMPERATURE = 1960.

 SUBROUTINE RECEIVER OUTPUT :

 ETARCM =  .88462008+00      RAM =  .30862879+00     QRECM =  .44305383+05

 SUBROUTINE ENGINE OUTPUT :

 ETAEM =  .37596992+00      RPCM =  .27999999+01     WNCM =  .43697739+02

 SYSTEM OUTPUT:

 TREC  =  .19600000+04      ETASY =  .33259054+00


*** END OF RUN ***
```